Order Number 8812834

The synchronous injection ignition valveless pulsejet

Smith, Dudley Edington, Ph.D.

The University of Texas at Arlington, 1987

U·M·I
300 N. Zeeb Rd.
Ann Arbor, MI 48106

PLEASE NOTE:

In all cases this material has been filmed in the best possible way from the available copy. Problems encountered with this document have been identified here with a check mark __✓__.

1. Glossy photographs or pages _____
2. Colored illustrations, paper or print _____
3. Photographs with dark background _____
4. Illustrations are poor copy _____
5. Pages with black marks, not original copy _____
6. Print shows through as there is text on both sides of page _____
7. Indistinct, broken or small print on several pages __✓__
8. Print exceeds margin requirements _____
9. Tightly bound copy with print lost in spine _____
10. Computer printout pages with indistinct print _____
11. Page(s) _____ lacking when material received, and not available from school or author.
12. Page(s) _____ seem to be missing in numbering only as text follows.
13. Two pages numbered _____. Text follows.
14. Curling and wrinkled pages _____
15. Dissertation contains pages with print at a slant, filmed as received __✓__
16. Other _____

_____

_____

THE SYNCHRONOUS INJECTION IGNITION VALVELESS PULSEJET

by

DUDLEY EDINGTON SMITH

Presented to the Faculty of the Graduate School of
The University of Texas at Arlington in Partial Fulfillment
of the Requirements
for the Degree of

DOCTOR OF PHILOSOPHY

THE UNIVERSITY OF TEXAS AT ARLINGTON

December 1987

THE SYNCHRONOUS INJECTION

IGNITION VALVELESS

PULSEJET

APPROVED:

Donald R. Wilson
(Supervising Professor)

D W Smith

S. R. Beard

Bob L. Perkin
(Dean of the Graduate School)

dedicated, with love, to my Debbie

ACKNOWLEDGMENTS

The author would like to thank Dr.'s D. D. Seath, K. L. Lawrence, A. Haji-Sheikh, and S. R. Bernfeld for their efforts in the review of the final draft and their many helpful suggestions. All of which have been greatly appreciated. Thanks are also due to Dr. B. R. Mullins for his assistance in the preparation of this paper.

I would especially like to thank Dr. D. R. Wilson for his patience and encouragement during this research. His guidance and support during this effort have been sincerely appreciated.

I would also like to thank the Department of Aerospace Engineering at The University of Texas at Arlington for their past support.

Finally, I would personally like to extend my love and thanks to my family for their love, understanding, and support, for without that, this would not have been possible.

November 23, 1987

THE SYNCHRONOUS INJECTION IGNITION

VALVELESS PULSEJET

Publication No._____

Dudley Edington Smith, Ph.D

The University of Texas at Arlington, 1987

Supervising Professor: Donald R. Wilson

An unsteady, quasi-one-dimensional channel flow code has been developed for the purpose of analyzing transient flow phenomena associated with the operation of valveless pulsejets. The method employs a real gas method-of-characteristics analysis, with discrete tracking of shock waves and other discontinuities. Frictional and heat transfer effects, as well as spatially varying cross sectional area are included in the analysis. The combustion transient is based on a hybrid, quasi-one-dimensional mixing, constant volume combustion model. The pulsed combustion model incorporates empirical turbulent mixing lengths of the injected fuel and a simple heat release model for the constant volume combustion process.

Comparisons of performance calculations and experimental data are presented for a selection of valveless pulsejet configurations. Calculations of mass flows,

temperatures, pressures, fuel consumption, thrust developed, and fuel air ratios as a function of the various geometries and fuel injection methods are in excellent agreement with existing experimental data.

Evaluation of the Synchronous Injection Ignition (SII) concept, which is the synchronized injection of a metered amount of high pressure fuel at the most advantageous point in the operating cycle of the device, instead of the present almost continuous injection during the whole cycle; via the calibrated analysis described above, indicates reduction in the specific fuel consumption on the order of 20% to 50% can be achieved for SII valveless pulsejets as compared to standard valveless pulsejets.

TABLE OF CONTENTS

LIST OF ILLUSTRATIONS

NOMENCLATURE

A	area
a	wave speed
C	Mach line
cv	control volume
cs	control surface
c_f	skin friction coefficient
c_H	Stanton number
c_p	specific heat at constant pressure
c_v	specific heat at constant volume
D	diameter
e_i	internal energy
F	thrust
f	frequency, force
H	specific heat value of fuel
h	enthalpy
I	impulse
k, K_1, K_2	constants
L, l	length
l'	effective length
M	Mach number
m	mass flow
$\dot{m}$	mass flow rate
mR	mixture ratio
n	exponent (constant) in eq. 3.1-21

p	pressure
q	heat transfer rate per unit area
R	gas constant
r	radius
S	cross sectional area
s	constant in eq. 2.4.3-3
T	temperature
t	time
u	mean velocity
V	velocity component, volume
x,y,z	cartesian coordinates
β	wall skin friction force
γ	ratio of specific heats
ε	wall roughness factor
η	shock determination factor, efficiency
$\lambda_{\pm}$	slope of Mach lines
λ_o	slope of path lines
μ	coefficient of viscosity
ν	constant in eq. 3.1-10, volume
π	constant (3.14159)
ρ	density
τ	shear stress
ω	circular frequency
Δ	step increment

subscripts

a	air
B	combustor
c	cycle
e	exit
f	fuel, final
H	hydraulic
i	initial, instantaneous
o	free stream, undamped
w	wall

CHAPTER 1

INTRODUCTION

1.1 Thesis Objective

The Synchronous Injection Ignition (SII) concept is that significant improvements in the performance of valveless pulsejets can be achieved via a synchronized, high pressure injection of a metered amount of fuel at the most advantageous point in the operating cycle of the device, instead of the present almost continuous injection of fuel during the whole cycle. The evaluation of the SII concept is the major objective of the present work.

To evaluate this concept, the following sub-objectives were required:

i) The development of a numerical model for the quasi-one dimensional, nonsteady flow, such as that which occurs in a valveless pulsejet. The numerical model should be able to take into account entropy gradients, area change, friction, heat transfer,and exothermic reactions (combustion) in the flow field, in addition to subsonic, sonic, and supersonic flow conditions.

ii) The development of a nonsteady combustion model to be incorporated into the above. The model should be able to simulate injection, atomization, mixing, and

ignition of the fuel spray as a function of fuel injection pressure, mass flow, combustion chamber pressure, and wave conditions.

iii) Calibration of the above simulation via comparison with existing experimental data. Analysis of various fuel injection schemes as well as combustion chamber geometry was essential.

iv) Evaluation of the feasibility of the SII concept as a means to significantly improve the specific fuel consumption of a standard valveless pulsejet via the calibrated simulation.

The SII concept is novel in that the proposed timed injection and metering of fuel in the valveless pulsejet is now possible. Previous investigators were limited in the possible schemes that could be proposed, given the existing technology, to improve the performance of the standard valveless pulsejet. Recent advances in computational capabilities and numerical analysis procedures when combined with the explosive developments in the micro-electronics industry, particularly in the area of automated controls, have made a reappraisal of this device possible. The application of new technology to the operation of the valveless pulsejet now allows for a more detailed analysis and the precise control of the device.

The major objective, the demonstration of the

feasibility of the SII concept, has been accomplished. The application of the SII concept indicates reductions of 20% to 50% in the specific fuel consumption relative to a standard valveless pulsejet can be achieved, thus making the SII valveless pulsejet competitive with other devices as a principal means of propulsion.

1.2 Historical Background

The idea of pulsed combustion appears to have preceded the use of steady state combustion as employed in gas turbine power generators. In the first decade of the twentieth century several pulsating gas generators appeared. The first schemes of air-breathing jet engines and gas turbines were conceived in the wake of the successful development of the reciprocating internal combustion engine. The extent to which this development determined the thought of jet propulsion is clearly evidenced in a scheme which was proposed by Lorin in 1908 (Ref. 1), where the combustion products of a reciprocating engine would be expanded through nozzles for the direct generation of thrust, letting the shaft be supplied with only the power required to produce compression and overcome losses (Fig. 1-1).

The first successful heat engine based on the wave process was the gas turbine of Holtzwarth (Ref. 2), but gas

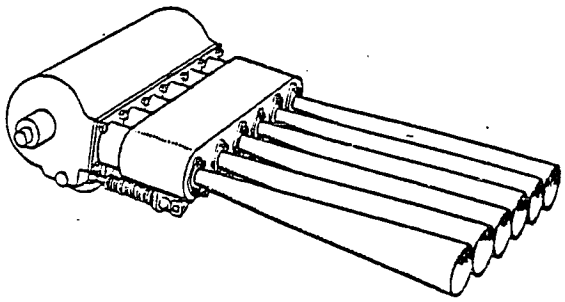

Figure 1-1 Lorin scheme of 1908

inertia effects were more fully utilized by Karavodine (Ref. 3), who in 1908 succeeded in driving a turbine by the means of gases exhausting through a long pipe from a resonating explosion chamber (Fig. 1-2). The inertia of the gas in the pipe was used not only for scavenging but also to permit the pressure to rise in the combustion chamber

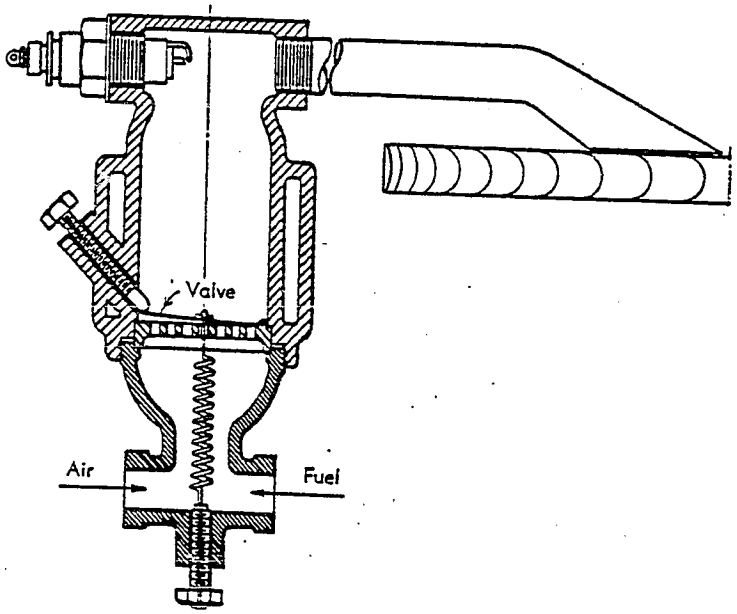

Figure 1-2 Karavodine turbine of 1908

during the charging process.

It is noteworthy that Marconnet (Ref. 4), having invented in 1909 a jet engine which was substantially a ramjet (Fig. 1-3), failed to recognize it for what it was and described it in his patents as operating intermittently.

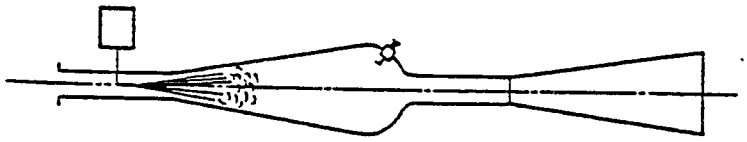

Figure 1-3 Marconnet jet engine of 1909

Marconnet later applied the concept of using the wave process similar to Karavodine to the direct generation of thrust. The result of this was Marconnet's now famous "reacture-pulsateur" (Fig.1-4) which was in every way the precursor of the modern day pulsejet.

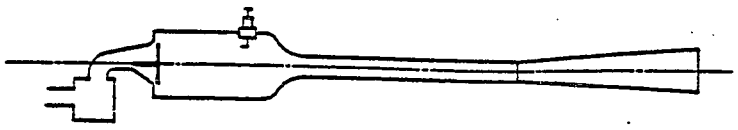

Figure 1-4 Marconnet's "reactor-pulsateur" of 1909

The utilization of pressure waves as a vehicle for the transfer of energy from the combustion products to the fresh charge for the purpose of precompression was attempted very early in the history of gas turbine development. The Esnault-Pelterie gas generator (Ref. 2) of 1913 utilized the pressure wave generated by the explosion at one end of a long combustion chamber to precompress the charge at the other end (Fig. 1-5).

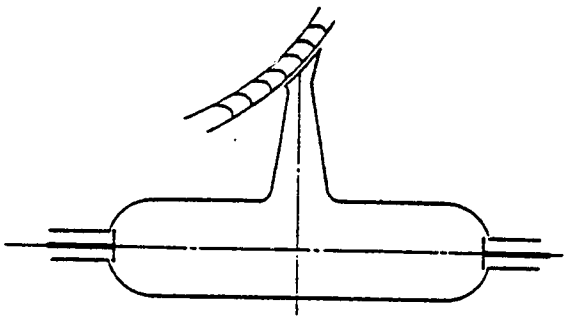

Figure 1-5 Esnault-Pelterie precompression engine of 1913

Application of the wave precompression concept as well as Marconnet's wave engine was revived by P. Schmidt. In 1930 and 1931 Schmidt described in a patent (Ref. 5) the intermittent pulsejet engine in its general form. While his development was directed toward its use in vertical take off and landing vehicles (Fig. 1-6), his major contribution to the development of the pulsejet was in the area of experiments demonstrating the principles of the ignition

process. His description of the shock wave ignition process, where the ignition velocities are on the order of several hundred meters per second, provided an insight to one of the distinct features of the pulsejet and its operation.

As the potential of the pulsejet as a direct thrust generator had been demonstrated (Fig. 1-7), development as a principle propulsion device was accelerated in the late 1930's and early 1940's.

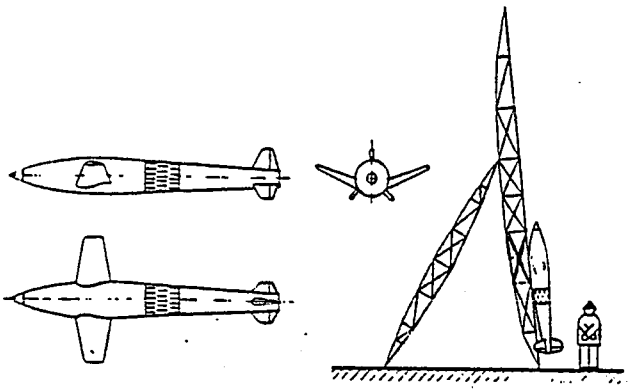

Figure 1-6 Schmidt VTOL project vehicle

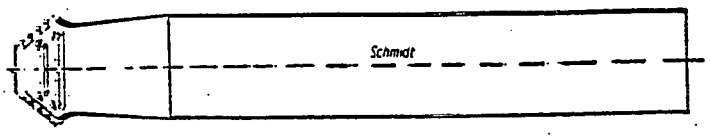

Figure 1-7 Schmidtrohr of 1931

In 1939 the German Air Ministry decided to have all forms of jet engines developed. The Argus Motoren Gesellschaft of Berlin was asked to develop a pulsejet. This project was under the direction of Dr. Fritz Gosslau. The development of the Argus pulsejet engine for the V-1 flying bomb was an independent development from that of P. Schmidt. It has been erroneously reported in numerous publications that the Argus work was in conjunction with P. Schmidt (Ref. 6). The Argus engine (Fig.1-8) which was used successfully on the V-1 was a simple valved pulsejet designed as a "disposable" system. Development work during the period from 1943 to 1945 in the area of fuel control and atomization led to speed increases and range increases of the V-1 (Fig. 1-9) from 600 km/hr to 800 km/hr, with no modification of the geometry of the jet itself.

It was also during this time period the first true systematic analytical approaches to the design and analysis of the operational cycle of the pulsejet were performed. In 1943 F. Schultz-Grunow published his paper "Gasdynamic Investigation of the Pulse-Jet Tube" (Ref. 7). Schultz-Grunow utilized the now familiar one-dimensional method of characteristics approach to the solution of the non-steady flow and wave motion in a tube.

Intelligence reports along with captured German V-1's spurred the United States to analyze and investigate

the pulsejet (Ref. 8). Researchers were brought together under Project Squid of the U. S. Navy. The analysis of the V-1 indicated large throttling losses due to the valve

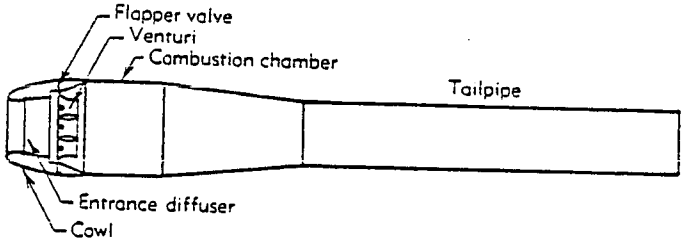

Figure 1-8 Argus V-1 pulsejet engine

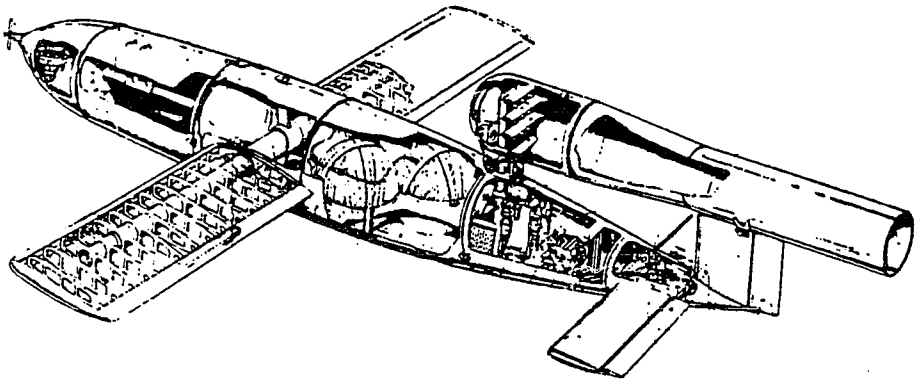

Figure 1-9 V-1 (Fi 103) flying bomb

bank. It was then suggested that the pressure losses could be eliminated or at least reduced to a minimum if the valves were dispensed with and rely on the resonance effect of the air and gas column to control the flow. The result is the valveless pulsejet as described by Schubert (Ref. 9) (Fig. 1-10).

Schubert along with Dunbar, Hussey, and Logan

developed the valveless pulsejet through systematic experimentation and limited analysis in the form described by Schultz-Grunow and expanded upon by G. Rudinger (Ref. 10). At that time period, 1945-1955, computational capabilities were limited and solutions were normally of the graphical type, with its inherit errors. The time required to calculate a few cycles for a fixed geometry normally exceeded several hundred man hours, thus limiting the analytical studies while the majority of the time concentrated on the experimental "cut-and-try" methods.

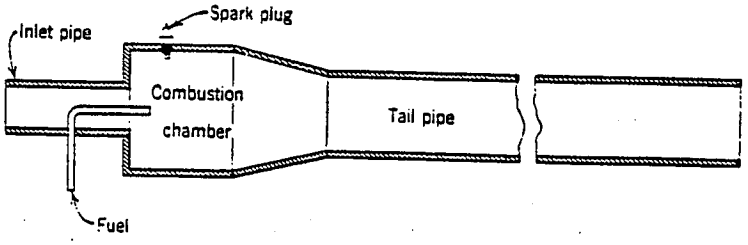

Figure 1-10 Valveless pulsejet of Schubert 1944

In the early 1950's, French engineers at SNECMA began their development of the valveless pulsejet (Ref. 11). The French were interested in applications in the areas of unmanned vehicles, such as drones and auxiliary propulsion devices for V/STOL aircraft. These French engineers are generally credited with the conception and development of the flow rectifier for valveless pulsejets (Ref. 12), to eliminate spillage of thrust in the intake by turning the

intake flow 180 degrees to coincide with the exhaust thrust. The general arrangement of these pulsejets can be seen in Figures 1-11 and 1-12.

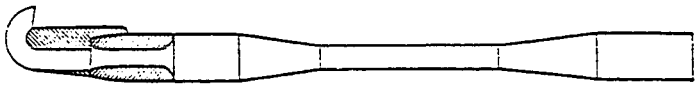

Figure 1-11 SNECMA valveless pulsejet ESCOPETTE

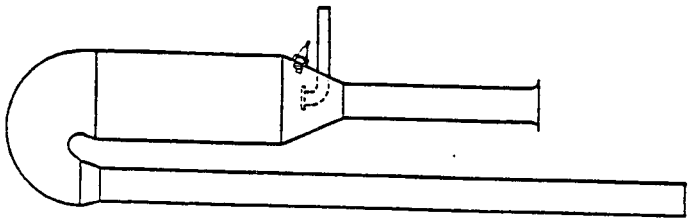

Figure 1-12 SNECMA valveless pulsejet ECREVISSE

Although not directly specified in their reports and publications, the major technical advance produced by the French research was the significant reduction in the specific fuel consumption of the standard valveless pulsejet through the intermittent injection of the fuel (Ref. 13). Through the use of low pressure fuel injection, the French were able to intermittently inject the fuel. As the pressure in the combustion chamber varied during the operating cycle, the supply of fuel to the combustion chamber was restricted and even terminated for a portion of the cycle as the combustion chamber pressure exceeded that of the

fuel injection nozzle. The result was a simple fuel injection control which led to a reduction in the specific fuel consumption. By intermittently injecting the fuel, instead of the previous practice of a continuous injection, large amounts of fuel which produced no useful thrust, but which were being expelled, were no longer injected. This novel approach was later used by Lockwood (Ref. 14), who described the operation and its effect in great detail.

While the low pressure injection scheme allowed fuel to be injected in an intermittent fashion with the use of an ultra simple device, which was necessary since the technology did not exist to achieve this in any other form, it presented its own limitations. The major disadvantages of a low pressure injection scheme are one, the precise timing of the injection, two the mixture control of the fuel injected and, three the atomization of the fuel for a more efficient combustion. Although Lockwood (Ref. 15) first described in detail the results of the intermittent injection on the fuel consumption of the valveless pulsejet, the credit for the approach should be yielded to the French. The French research, along with that of Lockwood, serves as the "proof of concept" of the basic idea which is the foundation of the Synchronous Injection Ignition concept, which is that by a synchronized injection of a metered amount of high pressure fuel at the most advantageous

point of the operating cycle instead of the present almost continuous injection during the whole cycle, a more efficient combustion and significant reduction in the specific fuel consumption can be achieved.

Until the late 1950's the concept lay dormant. R. Lockwood (Ref. 15) of Hiller Aircraft, at that time, with the support of the French researchers, began his extensive evaluation of the performance capabilities of valveless pulsejets. Lockwood's work is a landmark in the investigation of valveless pulsejet technology because it is the only completely documented, systematic study in existence. Lockwood, as previously noted, first described in detail the effects of low pressure-intermittent fuel injection as well as experimentally developed optimum configurations for combusters and jets. He also developed empirical scaling relationships and design procedures for the sizing and development of valveless pulsejets. Lockwood utilized analytical tools developed by Foa (Ref. 12). Foa's work in 1960 represented the most complete analytical approach available. Even so, the use of such analysis at the time was extremely tedious. Calculations of a few cycles for a given geometry required several hundred man hours, and then only incorporated the very simplest of gasdynamic models with no details of the combustion process.

Analytical evaluation of valveless pulsejets made its

most dramatic step forward since Schultz-Grunow's method of characteristics analysis with the publication in 1964 of C. E. Tharratt's summary paper of the results of a decade of development work by Saunders-Roe (Ref. 16). In his paper, Tharratt developed a heuristic approach by a linearization of a highly nonlinear problem. The resulting analysis, while not precise, gives surprisingly accurate results for most quantities of interest. It is a segmented analysis, that is portions of the operation of the jet are analyzed separately, therefore it is not as handy as one would wish for a design tool, but its application of fundamentals yields a physical understanding of the cycle operation superior to other analysis tools.

The most recent approaches to the development of valveless pulsejets are those of Kentfield and his associates at the University of Calgary in Canada (Ref. 17). These researchers efforts initially centered on the development of computer simulations of the cyclic operation of the valveless pulsejet, but their more recent activities have been in the experimental arena. The simulations had advanced to hot-flow type method of characteristics programs (Ref. 18) which were successful in predicting experimental results closely. However, the modeling is restricted to the tuned inlet and outlet geometries only and cannot predict combustion chamber geometric variations, fuel injection and

mixing, or the combustion process effects. As indicated in their own works,

> "further work is needed in order to model, correctly,.... valveless pulsed combustors .... and their geometry...." .

1.3 Relation to Valveless Pulsejet Technology

The development of the valveless pulsejet as a useful device has been restricted due to the nature of its operation. The geometry of the valveless pulsejet is the essence of simplicity, a device which has no moving parts but produces thrust! It relies on wave processes and the transfer of chemical energy, in the form of combustion, transferring this to a "momentum medium" that is discharged in the form of a directed jet. The process is unsteady with all possible forms of flow effects: combustion, friction, heat transfer, geometry, etc.

The complex nature of the gasdynamic operation of the valveless pulsejet has been the single most important aspect impeding its progress. Until the advent of advanced computers and more recently the development of numerical procedures for the analysis of these complex flow problems, the systematic analysis and design of these devices has been severely restricted. Researchers, until recently, had

to rely on the "cut and try" experimental approach, with their actions guided by "simplified component models". By the incorporation of these recent technical advances and the initial incorporation of a hybrid combustion model, the present research represents the first comprehensive model of the operation of the valveless pulsejet which will allow a systematic analysis of all components and aspects of the operation in a form suitable as a design tool. The analysis itself is the result of a progressive refinement of techniques previously developed and represents the logical extension of those past efforts to this time.

The present analysis draws heavily on the efforts of previous researchers in the defining of the fundamental operational limits and utilizes these as design constraints. Both theoretical and experimental values are incorporated in an effort to constrain the analysis to regions of actually demonstrated operations. Use of those limits and experimental results in the confirmation and calibration of the simulation result in an analysis capability which the present researcher believes is adequate to evaluate new concepts such as the Synchronous Injection Ignition concept.

The present research specifically differs in what has been done before in that it is the first simulation of the cyclic operation of the valveless pulsejet to incorporate a

hybrid combustion model which will allow for a systematic study of the operation inclusive of all components, including the intake, combustor, and exhaust geometries. The simulation is also unique in that within the combustion model is incorporated a fuel injection and mixing model to simulate various fuel input properties allowing for the study of those effects on the overall performance of the valveless pulsejet.

Therefore, the simulation developed by the present researcher represents the present state-of-the-art, in that all components, including the combustion process, are available for a systematic investigation in a complete form applicable as an engineering design tool.

1.4 Results and Possible Applications

The application of the present analysis to the Synchronous Injection Ignition concept indicates the concept to be a feasible means to improve the performance of the standard valveless pulsejet. Simulation of the concept, via the calibrated analysis, indicates a reduction in the specific fuel consumption of the SII valveless pulsejet over a standard, low pressure injection, valveless pulsejet to be on the order of 20% to 50%, depending on the size of the combustion chamber and its geometry. This reduction in the specific fuel consumption brings the performance of the

SII valveless pulsejet into competition with the turbojet. When combined with its simplicity of construction, operation, and inherent lower weight, The SII valveless pulsejet becomes a serious economic competitor in the commercial market. When viewed in the context of the primary gas generator for a turbine driving propellers, such as in the turboprop, and turbine driven fans, such as in the turbofan; the concepts, similar to Karavodine's application, of a "pulseprop" and "pulsefan" offer considerable promise to the SII valveless pulsejet as a principal propulsion device.

CHAPTER 2

THEORY OF VALVELESS PULSEJETS

2.1 Cyclic Operation of a Valveless Pulsejet

Consider the valveless pulsejet cycle diagram presented in Fig. 2-1. The first illustration (a) represents the starting sequence in which fuel, spark (or an ignition source), and a brief blast of starting air are turned on simultaneously.

As combustion occurs, the pressure builds up in the combustion chamber and the gases begin an expansion out of both ends of the combustor, that is from the inlet as well as from the tailpipe. As is shown in Fig. 2-1(b), the jets become well established, in that the chemical energy of the combustion, in the form of heat, generates the combustion chamber pressure rise, which in turn transfers momentum to the fluid medium, as the gas expands. The "slugs" of combustion products are then expelled from both the inlet and exhaust. Note, for low pressure fuel injection systems, about 10 pounds per square inch, the combustion chamber pressure, which is 30-45 pounds per square inch during this phase, exceeds the fuel pressure, therefore, the fuel flow is terminated while this condition remains in effect.

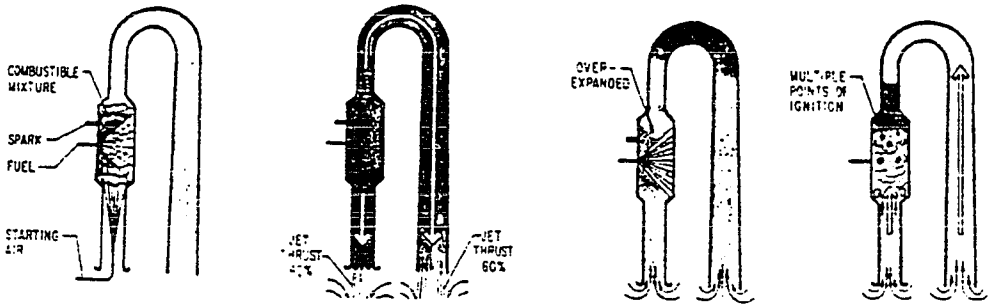

IGNITION AND COMBUSTION (a)	EXHAUST (b)	INFLOW (c)	PRE-COMBUSTION PRESSURE RISE AND MIXING (d)

Figure 2-1 Valveless pulsejet cycle diagram

Figure 2-1 (c) shows the combustion gases over-expanded. As the "slugs" of combustion products are accelerated away from the combustion chamber, the over expansion occurs and the pressure in the combustion chamber drops. The inertia of the "slugs" causes them to flow out of the inlet and the tailpipe with one-way piston-like action. Associated with the pressure drop there is a commencement again of the fuel flowing back into the combustion chamber and a reversal of air flow back into the inlet of the combustor and also up the tailpipe of low velocity air near these regions. As the tailpipe is of a much greater length than the inlet, the portion which was expelled was actually from the previous cycle. The shaded portion in the bend repre-

sents hot gases which did not leave during the first sequence. These hot gases are swept back into the combustion chamber where they are mixed with the fresh charge of fuel and air.

Consider figure 2-1(d), where the electrical ignition system is off. Ignition will occur at many points in the mixture due to the hot gases in the new charge. Where the mixture is stoichiometric, these hot gases provide ignition sources. The operation is now more efficient than in the starting cycle. Pressure in the combustion chamber is higher than in the situation where a single spark was used for ignition, because with multiple ignitors burning time is much reduced.

This vigorous mixing and stirring of the hot gases from the preceding cycle with fresh charge, combined with the ignition at multiple sources, is what makes this type of engine quite insensitive to the types of fuel used and explains why it can use a wide variety of fuels with little or no change in performance.

2.2 Summary of Existing Analytical Approaches

2.2.1 Helmholtz Resonator Analogy

The simplest analytical model of the valveless pulsejet is that of a Helmholtz resonator in combination with a

quarter wave oscillator. While the analogy is one of the simplest forms, it allows for a wealth of understanding of the fundamental operation of a valveless pulsejet. The model assumes that the combustion chamber and inlet can be modeled as a Helmholtz resonator and the exhaust as a matched, or tuned, quarter wave oscillator (the familiar pipe organ).

The Helmholtz resonator is a classic element in the study of acoustics (Refs. 19 and 20). In its simplest form the Helmholtz resonator can be described as a rigid enclosure of volume, V, communicating with the external medium through a small opening of radius, r, and length, ℓ, (Fig. 2-2). The gas in the opening is considered to move as a unit and provide the mass element of the system. The pressure of the gas within the cavity of the resonator changes as it is alternately compressed and expanded by the influx and efflux of gas through the opening and thus provide the stiffness element. At the opening, there is a radiation of sound into the surrounding medium, which leads

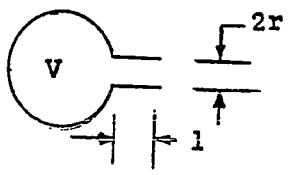

Figure 2-2 Simple Helmholtz Resonator

to the dissipation of acoustic energy and thus provides a resistance element .

The gas in the opening has a total effective mass of $\rho_o S\ell'$, where ρ_o is the density, S is the cross-sectional area of the opening, and ℓ' is its effective length. Since some of the gas beyond the end of the actual constriction moves as a unit with the gas in the constriction, it is necessary to use an effective length ℓ' which is greater than the true length. The value of ℓ' can be found by application of

$$\ell' = \ell + 2\,\Delta\ell \qquad 2.2.1\text{-}1$$

where $\Delta\ell$ the end correction varies given the geometry of the opening. Values of $\Delta\ell$ have been obtained (Ref. 19) mathematically for relatively low frequencies which give

$$\Delta\ell = 8\,r\,/\,3\,\Pi \approx 0.85\,r \qquad \text{flanged} \qquad 2.2.1\text{-}2$$

$$\Delta\ell \approx 0.6\,r \qquad \text{unflanged outlet} \qquad 2.2.1\text{-}3$$

Resonance of the Helmholtz resonator will occur when the acoustic reactance equals zero, or at

$$\omega_o = a\sqrt{\frac{S}{\ell' V}} \qquad 2.2.1\text{-}4$$

where a is the wave speed, and ω_o is the frequency of undamped free oscillation of the gas (no friction).

If we assume the frequency of the combustion chamber and inlet combination can be represented by the Helmholtz resonator, then we can match a tuned exhaust length to operate at the same frequency. The frequency of the tuned exhaust can be obtained from the linear theory which yields

$$f_o = \frac{a}{4\,L} \qquad 2.2.1\text{-}5$$

where L is the length of the tube (Ref. 20).

This simplified design approach yields quite good results and allows for the effect of intake diameter and length, combustion chamber volume and exhaust (or tailpipe) length variations. The result is that the specific thrust, as a function of combustion chamber volume and exhaust velocities and operating frequency, can be evaluated very accurately. The effects of the geometry variations can also be analyzed. If one begins with a given combustion chamber configuration, that is conical, straight, 45°, etc., the entire geometry and operation can be approximated to a high degree of accuracy and geometric variations and their gross effects evaluated quickly.

The above model is used in the present analysis as an initializer of the basic geometry and to provide a cross check on the operating frequency. For example, suppose a jet of a specific thrust level is under investigation.The size of the combustion chamber is determined from the

empirical scaling relationships and the initial geometry and approximate operating conditions are established using the Helmholtz resonator model. This approach has proven to help ensure a reasonable starting point in all simulations, and decreases substantially the time required to establish the range of variations to be evaluated in parametric evaluations and geometry optimization.

2.2.2 Control Volume Approach

The control volume approach which follows is attributed to Tao (Ref. 21), but it is known to others including the Germans who had similar developments (Ref. 6).

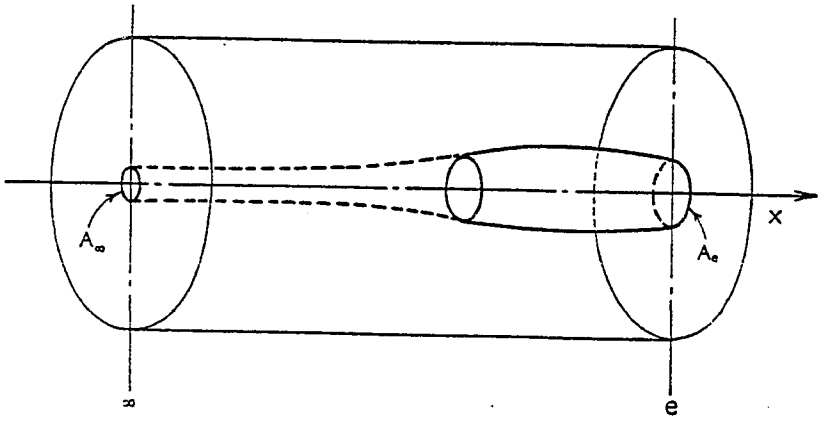

Figure 2-3 Control volume

Consider the cylindrical control surface (Fig. 2-3) enclosing the engine. The control volume extends upstream

and transversally to regions where the flow may be regarded as undisturbed and terminates at the exhaust station e. The velocity V is also assumed to be parallel to the free stream velocity V_∞ at all points of station e, and the static pressure p is assumed to be equal to the free stream static pressure p_∞ at all points of this station except in that portion which contains the exhaust jet (the area A_e), where the static pressure is p_e. Furthermore, the flow external to the engine is assumed to be isentropic and unaffected by the flow pulsations. This assumption implies the absence of frictional and wave drag and flow separation on the external surface of the engine. Then the instantaneous force acting in the positive x-direction on the flow region bounded by the control surface is

$$(p_\infty - p_e)\, A_e + F_i \qquad 2.2.2\text{-}1$$

where F_i is the instantaneous thrust produced by the engine. It also follows that the state and velocity of the external flow at all points of station e are the same as in the free stream. The momentum equation can then be written in the form

$$F_i - (p_e - p_\infty)\, A_e = \rho_e A_e V_e^2 - \rho_\infty A_\infty V_\infty^2 + \frac{\partial}{\partial t} \int_\tau \rho V d\tau \qquad 2.2.2\text{-}2$$

where τ is the volume of the internal flow region bounded by the control surface. The state and velocity are assumed to be uniform at each instant across the stated area.

The impulse I_c produced by the engine during one cycle of the periodic operation at a frequency f is obtained by a timewise integration of the previous equation over a period 1/f. In this integration, the term containing the volume integral vanishes because the flow is assumed to be periodic. Thus if we let

$$\int_{1/f} \rho_e V_e A_e dt = \frac{1}{f} \rho_\infty A_\infty V_\infty = m_c \qquad 2.2.2\text{-}3$$

and one neglects the mass flow of the fuel relative to the mass flow of the air, one gets

$$I_c = \int_{m_c} V_e dm - m_c V_\infty + \int_{1/f} (p_e - p_\infty) A_e dt \qquad 2.2.2\text{-}4$$

If we allow,

$$\bar{V} = \frac{1}{m_c} \int_{m_c} V \, dm \qquad 2.2.2\text{-}5$$

$$F = f I_c \qquad \text{(average thrust)} \qquad 2.2.2\text{-}6$$

$$\dot{m} = f m_c \qquad \text{(mass flow rate through engine)} \qquad 2.2.2\text{-}7$$

one obtains

$$F = \dot{m} (V_e - V_\infty) + f \int_{1/f} (p_e - p_\infty) A_e \, dt \qquad 2.2.2\text{-}8$$

now let,

$$\dot{m} V_e + (p_e - p_\infty) A_e = \phi \dot{m} V_x \qquad 2.2.2\text{-}9$$

where the subscript x denotes the flow conditions that would be established at the exit if the exhaust were fully expanded. A quasi-steady isentropic expansion of the exhaust flow from $p = p_e$ to $p = p_\infty$ would produce

$$T_e + \frac{V_e^2}{2 c_p} = T_e \left(\frac{p_\infty}{p_e} \right)^{\frac{\gamma-1}{\gamma}} + \frac{V_x^2}{2 c_p} \qquad 2.2.2\text{-}10$$

where T denotes the static temperature, or

$$\frac{V_x}{V_e}^2 = 1 + \frac{1 - \frac{p_\infty}{p_e}^{\frac{\gamma-1}{\gamma}}}{\frac{\gamma-1}{\gamma} M_e^2} \qquad 2.2.2\text{-}11$$

therefore,

$$\phi = \frac{\dot{m} V_e + (p_e - p_\infty) A_e}{\dot{m} V_x}$$

Then,

$$\phi = \left[1 + \frac{1 - \left(\frac{p_\infty}{p_e}\right)^{\frac{\gamma-1}{\gamma}}}{\frac{\gamma-1}{2} M_e^2}\right]\left[1 + \frac{1 - \frac{p_\infty}{p_e}}{\gamma M_e^2}\right] \qquad 2.2.2\text{-}12$$

Although the maximum thrust is obtained by a complete expansion, which can seldom be maintained in a nonsteady flow, the value of ϕ is so close to unity that the exhaust is generally treated as completely expanded. Equation 2.2.2-4 and 2.2.2-8 then reduce to

$$I_c = m_c \ (\bar{V}_x - V_\infty) \qquad 2.2.2\text{-}13$$

$$F = \dot{m} \ (\bar{V}_x - V_\infty) \qquad 2.2.2\text{-}14$$

The result is that, given an estimate of the mass flow rate through the engine and an estimate of the average or mean exhaust velocity, estimates of the upper limit of the specific impulse and thrust can be determined. Note that only gross effects are predicted, with no detailed information available from this analysis. Only the last two equations have been used in the analysis. From the information developed in the Helmholtz resonator model, the equations above are used to verify the results of the scaling rela-

tions relative to the generated model.

2.2.3 Fundamental Gas Dynamic Model

A simplified theory of the operation of pulsejets was developed by Tsien (Ref. 22). A basic overview of the theory is as follows.

Let the subscript o denote quantities corresponding to the free stream atmospheric conditions, the subscript 1 denote the conditions at the inlet, the subscript 2 denote the conditions in the combustion chamber at the end of the charging process and the subscript 3 denote the conditions at the end of combustion. Since the compression from free stream to the stagnation pressure is the same as the inverse of the isentropic expansion, the chamber conditions are now the stagnation conditions, and the exit are the free stream conditions. Thus for the above, we have

$$\frac{p_1}{p_o} = \left(1 + \frac{\gamma-1}{2} M_o^2\right)^{\frac{\gamma}{\gamma-1}} \qquad 2.2.3\text{-}1$$

The temperature ratio is then

$$\frac{T_1}{T_o} = 1 + \left(\frac{\gamma-1}{2}\right) M_o^2 \qquad 2.2.3\text{-}2$$

Since there is a pressure drop through the intake venturi, one can assume (for a valved jet)

$$P_2 = \frac{1}{2} P_1 \qquad 2.2.3\text{-}3$$

This basically assumes a dynamic pressure loss through the valve bank of one-half the inflow value. The temperature T_2, being representative of the total energy of gas at rest, must be the same as T_1, since no heat loss is assumed to occur, therefore

$$T_2 = T_1 \qquad 2.2.3\text{-}4$$

If one assumes that the combustion is carried out at constant volume, and if the small addition of the fuel flow is neglected, the heat added per unit mass of air is

$$h = c_v' (T_3 - T_2) = \frac{1}{\gamma'} c_p' T_3 \left(1 - \frac{T_2}{T_3}\right) \qquad 2.2.3\text{-}5$$

where the primes refer to the combustion products. For a constant volume combustion

$$\frac{T_2}{T_3} = \frac{p_2}{p_3} \qquad 2.2.3\text{-}6$$

Therefore

$$h = \frac{1}{\gamma'} c_p' T_3 \left(1 - \frac{p_2}{p_3}\right) \qquad 2.2.3\text{-}7$$

If one assumes that the rapid discharge can be approximated by a slow discharge of the same impulse, then one can assume an isentropic steady expansion of the combustion chamber pressure p to p_o, the atmospheric pressure. If the discharge velocity is assumed to correspond to p, then

$$V = \left(\frac{2\gamma'}{\gamma'-1} \frac{p}{\rho} \left[1 - \left(\frac{p_o}{p} \right)^{\frac{\gamma-1}{\gamma}} \right] \right)^{1/2} \qquad 2.2.3\text{-}8$$

The impulse due to a discharge of dm at this velocity is

$$dI = v\, dm \qquad 2.2.3\text{-}9$$

If the mass before removal of dm is m, then the ratio of the density in the chamber after removal of dm to that before is

$$\frac{m - dm}{m}$$

Similarly the pressure ratio is

$$\frac{p + dp}{p}$$

and since we assume the process to be isentropic, we have

$$\frac{p + dp}{p} = \left(\frac{m - dm}{m} \right)^{\gamma} \qquad 2.2.3\text{-}10$$

Neglecting higher order terms, one obtains

$$\gamma \frac{dm}{m} = \frac{-dp}{p} \qquad 2.2.3\text{-}11$$

This last equation shows that a discharge dm will decrease the pressure in the chamber, as expected. Since $m = \rho V$, where V is the volume of the combustion chamber, one can replace the dm in the impulse equation (2.2.3-9) by dp to yield

$$dI = - \left(\frac{2\gamma'}{\gamma'-1} \frac{p}{\rho} \left[1 - \left(\frac{p_o}{p} \right)^{\frac{\gamma'-1}{\gamma'}} \right]^{1/2} \right) \frac{1}{\gamma'} \rho V \frac{dp}{p} \qquad 2.2.3\text{-}12$$

Finally integrating eq. 2.2.3-12 from the initial pressure to the final pressure to find the total impulse due to the discharge,

$$I = \frac{1}{\gamma'} \sqrt{\frac{2\gamma'}{\gamma'-1}} V \int_{p_o}^{p_3} \sqrt{\frac{p}{\rho} \left[1 - \left(\frac{p_o}{p} \right)^{\frac{\gamma'-1}{\gamma'}} \right] \left(\frac{\rho}{p} \right)} \, dp \qquad 2.2.3.13$$

or,

$$I = \frac{1}{\gamma'}\sqrt{\frac{2\gamma'}{\gamma'-1}}\ (Vq3)\sqrt{\frac{p_3}{\rho_3}}$$

$$\times \int_{p_o/p_3}^{1} \left\{ \frac{1}{\eta^{\frac{\gamma'-1}{\gamma'}}} \left[1 - \left(\frac{p_o}{p_3}\right)^{\frac{\gamma'-1}{\gamma'}} \frac{1}{\eta^{\frac{\gamma'-1}{\gamma'}}} \right] \right\}^{1/2} d\eta$$

where $\eta = p/p_3$. Since $V\rho_3$ is the total mass in the combustion chamber at the beginning of the discharge, and

$$\gamma' \frac{p_3}{\rho_3} = a_3 \qquad 2.2.3\text{-}14$$

is the local speed of sound corresponding to the conditions in the combustion chamber at the end of combustion, the "effective velocity" V_e can then be defined by

$$\frac{V_e}{a_3} = \frac{1}{\gamma'}\sqrt{\frac{2\gamma'}{\gamma'-1}} \int_{p_o/p_3}^{1} \frac{1}{\eta^{\frac{\gamma'-1}{\gamma'}}} \left[1 - \left(\frac{p_o}{p_3}\right)^{\frac{\gamma'-1}{\gamma'}} \frac{1}{\eta^{\frac{\gamma'-1}{\gamma'}}} \right]^{\frac{1}{2}} d\eta \qquad (2.2.3\text{-}15)$$

For a unit mass flow per second, the thrust can be expressed by

$$1\ (V_e - V_o)$$

where V_o is the flight velocity and V_e is given by an expansion of 2.2.3-15 into a series for numerical evaluation, using $\gamma' = 4/3$ yields (to three terms)

$$\frac{V_e}{a_3} = \frac{6\sqrt{6}}{7}\sqrt{1 - \left(\frac{p_o}{p_3}\right)^{\frac{1}{4}}}\left[1 - \frac{1}{5}\left(\frac{p_o}{p_3}\right)^{\frac{1}{4}} - \frac{4}{15}\left(\frac{p_o}{p_3}\right)^{\frac{1}{2}} - \frac{8}{15}\left(\frac{p_o}{p_3}\right)^{\frac{3}{4}}\right] \qquad (2.2.3\text{-}16)$$

If the specific heat value of the fuel is given by H and η_B is the combustion efficiency, the specific fuel consumption becomes

$$S = \frac{3600\ h}{778\ H\ \eta_B\ (V_e - V_o)} \qquad 2.2.3\text{-}17$$

Substituting the value of h from 2.2.3-7, we get

$$S = \frac{3600\ a_3\ \ (1 - p_2/p_3)}{778\ H\ \eta_B\ (V_e/a_3 - M_o\ (a_o/a_3)} \quad \frac{1}{\gamma'(\gamma'-1)} \qquad 2.2.3\text{-}18$$

where the ratio of the sound velocities is given by

$$\left(\frac{a_3}{a_o}\right)^2 = \frac{\gamma' R' T_3}{\gamma R T_o} = \frac{c_p'}{c_p} \frac{\gamma'-1}{\gamma-1} \left(\frac{p_3}{p_2}\right) \left(\frac{T_1}{T_o}\right) \qquad 2.2.3\text{-}19$$

Thus the specific fuel consumption can be approximated if the combustion chamber pressure ratio and combustion efficiency can be determined.

This simple theory is based on a quasi-steady discharge and assumes the combustion chamber pressure ratio was on the order of unity, therefore the pressure variations are assumed to be small. Thus the basic approach was to use the linear theory of small perturbations. Additionally, the model fails to predict the operating frequency which is directly connected to the pulsating flow. However the prediction of the exit velocity ratios and the specific fuel consumption are useful in defining operating limits and are used as checks within the prediction model.

As can be seen, by this brief discussion of the simplified approach, the number of approximations, which indicate a number of unknown quantities, are difficult to estimate and the analysis is also segmented. The approach was developed from the experimental observations and techniques available at the time and represented a marked improvement over the control volume analysis as many more

physical details of the flow were included.

2.2.4 Linearized Theory

The next major improvement to the analysis of the operating cycle of the valveless pulsejet was a basic attempt to improve on the fundamental gasdynamic model by incorporating a simplified combustion model with the operations timed to generate the frequency information.

The operation of the pulsejet was broken into three distinct operations; charging, combustion, and discharging. For a given combustion chamber volume, assuming isentropic conditions, etc., as before in the fundamental gasdynamic analysis, the pressure as a function of time and thus the charging time could be found. To determine the combustion action, a control volume analysis of the combustion chamber was then used with timed heat release and chemical-kinetics equations to simulate the temperature rise and thus pressure rise in the combustion chamber, again, as a function of the time of the process. The cycle analysis was then completed with an expansion and discharge analysis of the combustion products as a function of time. This combination completed one cycle and thus yielded similar results as the fundamental approach, but with added capabilities. This "segmented" process was the first to separate the

combustion process and its effect into its own analysis. It also incorporated the calculation of the time of each operation, therefore tying the physical operation to the operating cycle. The frequency of operation being the reciprocal of the sum of the individual operation's times.

An excellent paper which describes this approach in detail as well as many related topics can be found in C.E. Tharratt's works (Ref. 16).

2.2.5 Quasi-One-Dimensional Method of Characteristics

The original method-of-characteristics analysis was done by F. Schultz-Grunow (Ref. 7). His original work was the gas-dynamic investigation of the operation of the pulsejet with studies on the effects of the form of the tube, variation of the cross-sectional area, speed of flight, and a description of the pressure changes in the combustion chamber.

Schultz-Grunow's approach was the graphical solution technique to the one-dimensional flow through the pulsejet tube. His studies included tubes of straight and conical shapes as well as combinations of the same. The work demonstrates reasons for many observed effects such as combustion chamber geometry relative to the intake and exhaust geometry, variation of cycle time with the combustion chamber as well as exhaust geometries, and the effects

on operation or non-operation relative to cross-sectional area variations.

Schultz-Grunow was the first to demonstrate analytically the re-ignition process via the condensation shock reflected within the exhaust.

Kentfield and his associates (Ref. 17) utilized a numerical procedure in the form of a method-of-characteristics solution. The appropriate hyperbolic differential equations of continuity, energy and momentum were solved simultaneously in a time dependent flow field. Through successive refinements, the effects such as area variation, hot flow, and combustion reaction rates have been incorporated. Although capable of handling combustion chamber geometry variations, Kentfield's associates limited their application of the method to the intake and exhaust tubes, analyzing the combustion chamber via a control volume approach.

The method-of-characteristics approach yields for the first time a unified approach to the modeling of the cyclic operation of the pulsejet. The ability to examine all phases of the operation, inclusive of geometries, allow for the development of a design as well as analysis tool.

2.3 Summary of Existing Approaches and a Comparison of their Attributes and Deficiencies

The existing analytical approaches to the solution of the cyclic operation of a valveless pulsejet fit in one of four categories. These categories are:

I. Acoustic Analogy

II. Control Volume Analysis

III. Fundamental Gasdynamics

IV. Linearized Theory

V. Method of Characteristics

For the acoustic analogy:

Attributes	Deficiencies
- simple rapid analysis with accurate results	- depends on empirically determined sizing constraints, contain no details as to the actual combustion process

Control volume analysis:

Attributes	Deficiencies

- simple analysis	- depends on time averaged values
	- yield only "gross" information
	- no details as toeffects
	  - combustion process
	  - frequency of operation
	  - fuel flow

Gasdynamic fundamentals:

Attributes	Deficiencies
- explains some basic physical phenomena	- no shape effects - no inclusion of frequency of operation - slow discharge assumption inadequate

Linearized Theory

Attributes	Deficiencies
- explains the basic physical phenomena - frequency of operation	- no shape effects - segmented analysis

Method-of-characteristics

Attributes	Deficiencies
- unified approach - geometry variation - frequency of operation - details of operation	- extremely difficult analysis

To develop a complete picture of the operation of a valveless pulsejet, and to serve as a design tool, the only choice in the analytical approaches is the method-of-characteristics. When combined with a sufficient combustion model, the ability to analyze and design the valveless pulsejet becomes possible.

2.4 Development of One-Dimensional, Transient, Gas-dynamic Model

2.4.1 General Description of the Flow System

The model employed in this paper is based on a quasi-one-dimensional, unsteady method of characteristics analysis which was developed by Wilson and Stewart (Ref. 23) for the analysis of transient magnetohydrodynamic power channels and diffusers. Detailed discussions of code development including evaluation of shock-fitting and shock-capturing methods,numerical integration algorithm selection, Lax-Wendroff analysis for interior points, and code validation can also be found in Ref. 23.

The basic analysis geometry for a valveless pulsejet consist of an intake, combustor, and exhaust (Fig. 2-4)

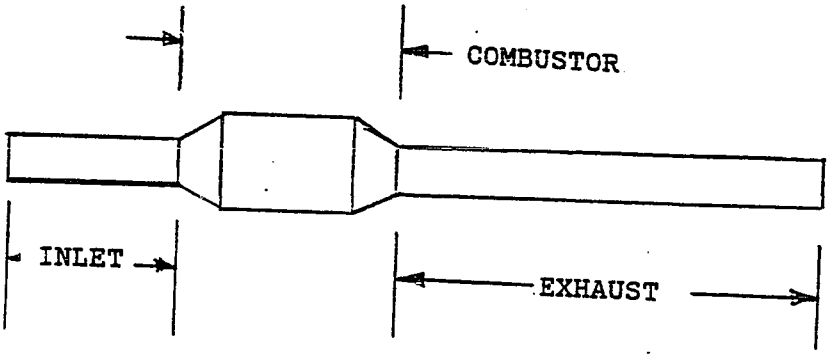

Figure 2-4 Valveless pulsejet geometry

The coordinate system for the flow geometry is shown in Figure 2-5. This coordinate system is used rigorously in the analysis and subsequent computer code. Note that the origin of the system is fixed at the location in the combustion chamber where the combustion ignition occurs. As the ignition point varies from cycle to cycle, as a function of fuel flow and other variables, the analysis of that cycle will be based upon the fixed system at the beginning of the cycle.

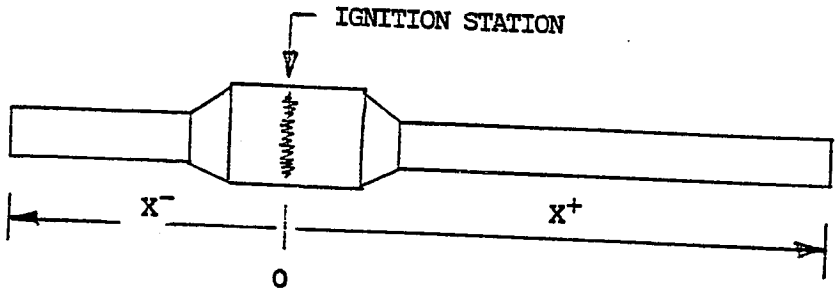

Figure 2-5 Coordinate system

Since the original code was established to analyze a single channel, the logic was generated to perform two separate analyses for the valveless pulsejet; one for the intake and one for the exhaust. For the coordinate system shown, the axial velocity is along the x-direction.

The Eularian forms of the basic conservation equations for a quasi-one-dimensional, unsteady flow (references 24,

27) are as follows:

continuity equation,

$$\frac{D\rho}{Dt} + \rho \frac{\partial u}{\partial x} + \frac{\rho u \, dA}{A \, dx} = 0 \qquad 2.4.1\text{-}1$$

momentum equation,

$$\rho \frac{\partial u}{\partial t} + u \frac{\partial u}{\partial x} = - \frac{\partial P}{\partial x} + \beta \qquad 2.4.1\text{-}2$$

where,

$$\beta = - \frac{4 \tau_w}{D_H}$$

energy equation,

$$\rho \frac{Dh}{Dt} - \frac{Dp}{Dt} = \Psi \qquad 2.4.1\text{-}3$$

where,

$$\Psi = \frac{4 u \tau_w}{D_H} + \frac{4 \dot{q}_w}{D_H}$$

Real gas thermodynamic properties used in the above equations are assumed to be explicit functions of pressure

and temperature,

$$\begin{aligned} \rho &= \rho(p,T) \\ h &= h(p,T) \\ a &= a(p,T) \end{aligned} \qquad 2.4.1\text{-}4$$

The wall shear stress τ_w is replaced by

$$\tau_w = c_f \frac{1}{2} \rho u^2 \qquad 2.4.1\text{-}5$$

where the skin friction coefficient is obtained by a Newton-Raphson solution of the Colebrook equation for turbulent duct flow, as done by Lee (Ref. 25) for Re > 2000,

$$\frac{1}{4 c_f} = -2 \log_{10} \left(\frac{\varepsilon/D}{3.7} + \frac{2.51}{Re\sqrt{4 c_f}} \right) \qquad 2.4.1\text{-}6$$

and directly from the Poiseuille flow equation (Ref.26) for laminar flow (Re < 2000),

$$4 c_f = \frac{64}{Re} \qquad 2.4.1\text{-}7$$

Wall convection heat transfer rates are calculated from

$$\dot{q}_w = C_H \rho u (h_o - h_w) \qquad 2.4.1\text{-}8$$

where C_H is calculated from an appropriate Reynolds analogy expression (Ref. 26).

$$C_H = \frac{c_f}{2} \qquad 2.4.1\text{-}9$$

2.4.2 Method of Characteristics

All phenomena in the flow field, including discontinuities (shock waves, contact surfaces) and their associated interactions and reflections are calculated by means of a modification of the inverse method of characteristics developed by Zuckow and Hoffman (Ref. 27). Instead of the classical approach, which uses velocity, pressure, and density as primary integration variables, the modified approach is based on the use of velocity, pressure, and temperature. This allows, if desired, the use of real-gas thermodynamic property tables, such as those generated by the NASA CEC76 code (Ref. 28), in which all thermodynamic properties are generated as explicit functions of pressure and temperature.

An inverse numerical method was generated to solve the compatibility equations

$$dp^{\pm} \pm \rho\, a\, du_{\pm} = \left(- \frac{\rho\, u\, a^2 dA}{A\, dx} \pm a\, \beta - \frac{1}{\rho\, c_p} \frac{\partial p}{\partial T} a^2 \Psi \right) dt_{\pm} \qquad (2.4.2\text{-}1)$$

along the Mach lines, whose slopes are given by

$$\lambda_{\pm} = \left(\frac{dt}{dx}\right)_{\pm} = \frac{1}{u \pm a} \qquad 2.4.2\text{-}2$$

and

$$\frac{u\,T}{\rho}\left(\frac{\partial p}{\partial t}\right)_p dp + \rho\, u\, c_p\, dT = \Psi\, dx \qquad 2.4.2\text{-}3$$

along the path line, with slope

$$\lambda_o = \left(\frac{dt}{dx}\right)_o = \frac{1}{u} \qquad 2.4.2\text{-}4$$

The detailed derivation of these equations is given in Reference 29.

The geometry of the calculational procedure for each direction of the flow, is illustrated in Figure 2-6.

The description of the calculation procedure for shock and contact discontinuities will be presented in Section 2.4.4.

To ensure that the solution is stable, the Courant-Friedrich-Lewy (CFL) stability criterion (Ref. 27) must be satisfied. The criterion requires that the initial data points (points 1, 2, and 3 in Figure 2-6) fall between the

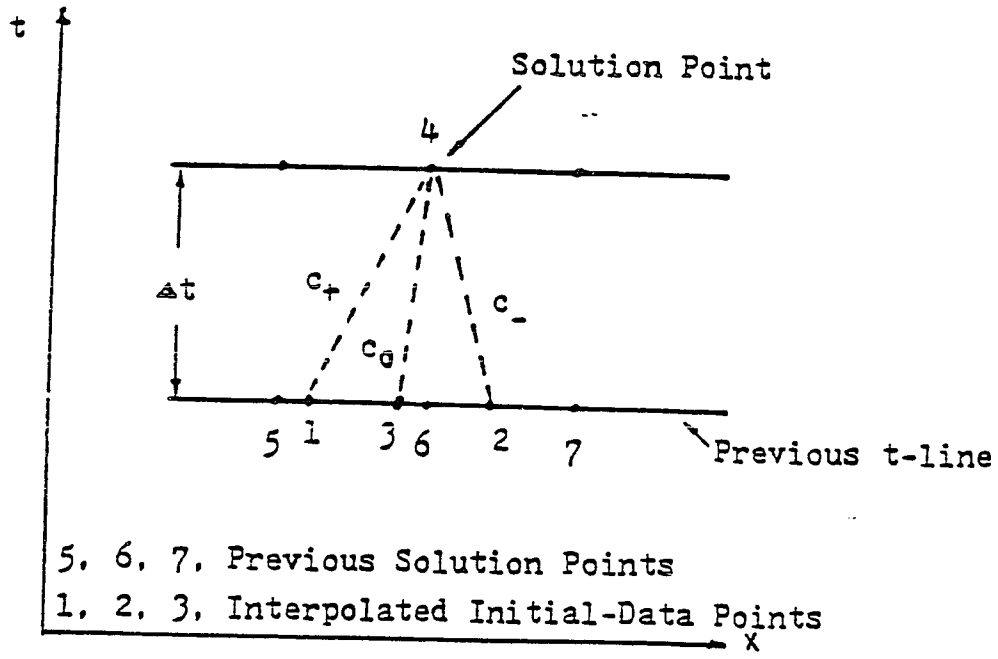

Figure 2-6 Finite difference grid for interior points

previous solution points (points 5, 6, and 7) that are employed in the interpolation for determining the flow properties at points 1, 2, and 3. In other words, if the time and distance increments remain fixed, the relationship

$$(u + a)_{max} \Delta t < \Delta x \qquad 2.4.2\text{-}5$$

must be satisfied to ensure the solution is stable.

2.4.3 Thermodynamic/Transport Properties

As employed by Wilson, Stewart, and Lee (Ref. 29), to reduce computer time, a perfect (thermal and caloric) gas model was employed for the calculation of the thermodynamic

properties needed for the calculations in this dissertation. With this assumption, the equation of state can be written as,

$$\rho = \frac{p}{(R/m)\ T} = \frac{p}{R\ T} \qquad 2.4.3\text{-}1$$

and the derivatives appearing in the compatibility equations are:

$$\left(\frac{\partial \rho}{\partial T}\right)_p = -\frac{p}{R\ T^2} \qquad 2.4.3\text{-}3$$

$$\left(\frac{\partial \rho}{\partial T}\right)_T = -\frac{p}{R\ T}$$

For more realistic solutions, real gas thermodynamic property tables, such as those generated by the NASA CEC76 computer code (Ref. 28), could be used. The values in the above tables are stored in a form as m = m(p,T) and can be extracted by tabular interpolation.

The coefficient of viscosity μ, needed in the friction factor calculations is obtained by Sutherland's law (Ref. 26) for the perfect gas solutions.

$$\mu = \mu_o \left(\frac{T}{T_o}\right)^{3/2} \frac{T_o + S}{T + S} \qquad 2.4.3\text{-}3$$

For real gas calculations, μ is obtained by tabular interpolation from tables generated by the NASA TRAN72 code (Ref. 30).

2.4.4 Shock Fitting Procedure

In order to match downstream boundary conditions, a standing normal shock wave can usually be found in the inlet or exhaust flows. The shock formation is normally the result of the combustion transient and moves to a position that is dictated by the upstream and downstream boundary conditions. The movement of the shock depends upon a number of factors, the most important being the transient combustion characteristics.

The most difficult aspect of the shock calculation for an inverse characteristic analysis is the development of a method to predict when and where the shock will be formed. By using a concept based on coalescence of characteristics (Ref. 31), a method can be developed that requires information on only 2 preceding nodal points. The method is both fast and reliable (Fig. 2-7).

In Figure 2-7, assume that the flow field is known at the i-th time step for every nodal point. The slope of the Mach lines at each nodal point are:

$$\lambda_j^{\pm} = \frac{1}{u_j \pm a_j} \qquad 2.4.4\text{-}1$$

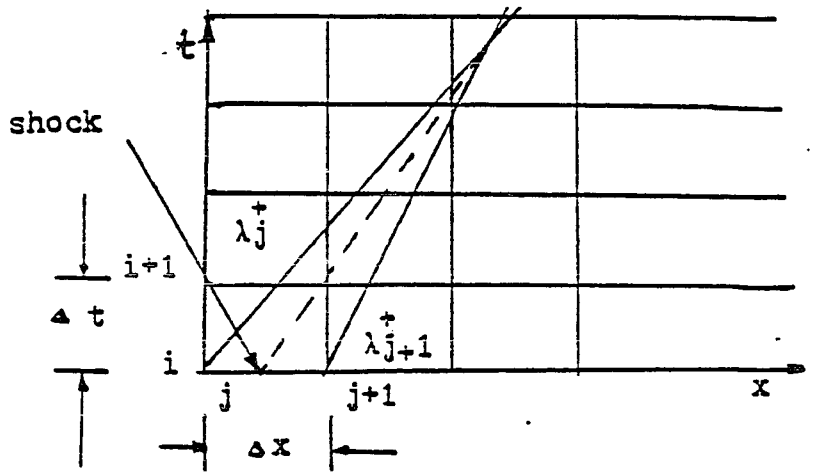

Figure 2-7 Shock detection

The values $\eta^{\pm}$ are defined as

$$\eta^{\pm} = \frac{(\lambda^{\pm}_{j+1} - \lambda^{\pm}_{j})(\Delta t)}{(\lambda^{\pm}_{j+1})(\lambda^{\pm}_{j})(\Delta x)} \qquad 2.4.4\text{-}2$$

which are the reciprocal of the number of steps needed for 2 adjacent characteristics to coalesce. For a fixed value of Δx, coalescence of characteristics is within four time steps for a value of $\eta^{\pm} > 0.22$. The value was found by Salas (Ref. 31) to fit a wide range of problems. For a value of $\eta^{\pm} < 0.22$, Salas found the procedure to become very sensitive, with the shocks predicted prematurely.

In general for flow from left to right, the shock wave may be classified as either right-facing or left-facing, depending upon whether the fluid particles enter the shock wave from the right or the left, respectively, as time

increases (Ref. 27). As far as the computational method is concerned, an easier way to examine if the shock is right-facing or left-facing is to examine the values of p_2 and p_1 on both sides of the shock wave (Figure 2-8). If $p_2 > p_1$, the shock is left-facing, otherwise the shock is right facing.

From equations 2.4.4-1 and 2.4.4-2, $\eta^{\pm}$ can be written as

$$\eta^{\pm} = \frac{\Delta t}{\Delta x} \{(u_j \pm a_j) - (u_{j+1} \pm a_{j+1})\} \qquad 2.4.4\text{-}3$$

For constant $\Delta t/\Delta x$, if $a_j > a_{j+1}$, the value of η^+ will exceed 0.22 before η^-, but for $a_{j+1} > a_j$, η^- will exceed 0.22 first. From this discussion we know that a_{j+1} will be less than a_j in a right-facing shock, and a_j will be less than a_{j+1} in a left-facing shock, thus equation 2.4.4-3 can be used to determine both when a shock will be formed and whether it is left- or right-facing. In order to prevent a large number of unnecessary calculations, weak shocks will be removed from the calculation by examination of η. If either $\eta+$ or $\eta-$ drops below 0.10, then the shock wave is removed and a small amplitude compression wave replaces the shock. This can then be tracked by the interior point routines. The value of $\eta^{\pm} = 0.10$ corresponds to a shock Mach number of 1.3, for which the pressure ratio p_2/p_1 is 1.70.

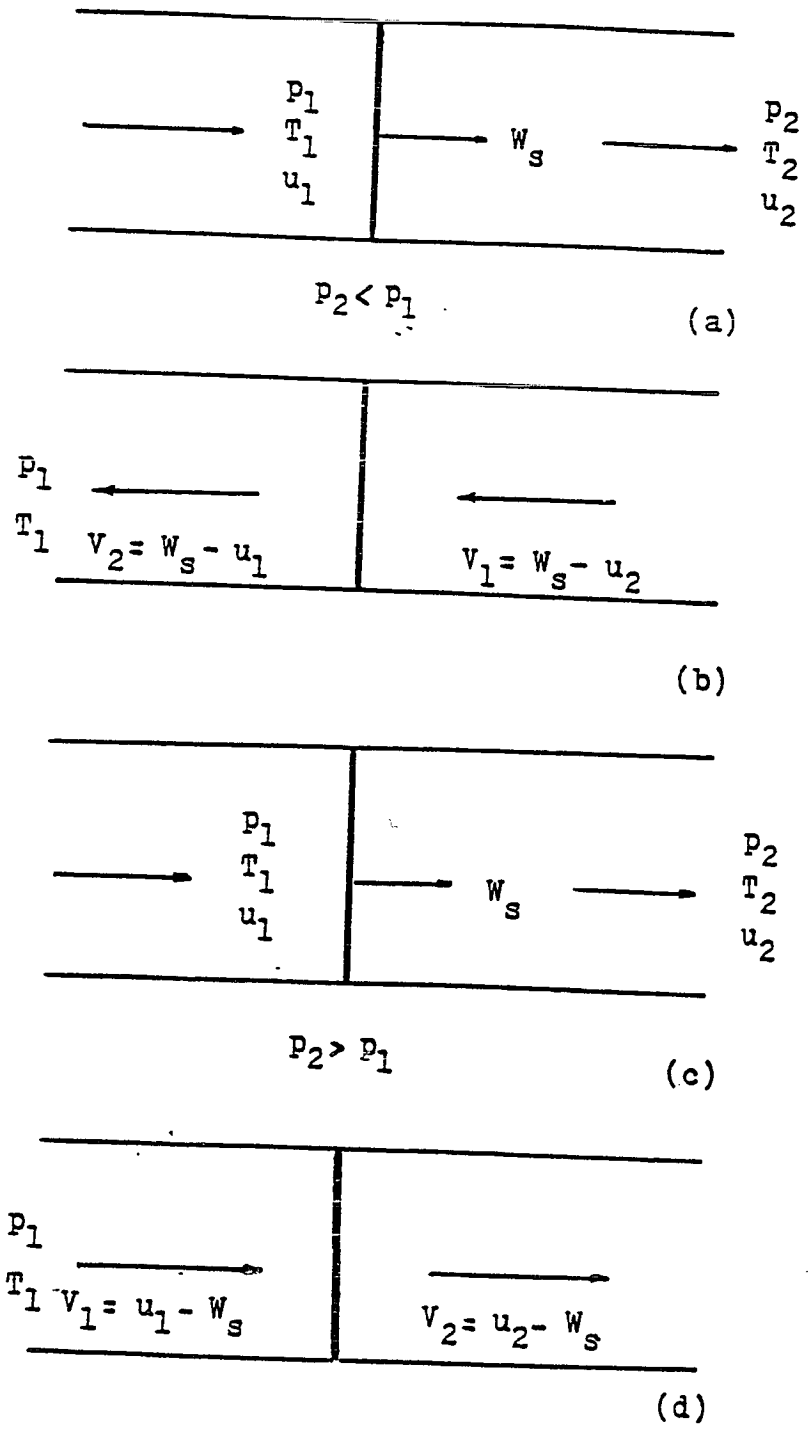

Figure 2-8 Transformation of a moving shock wave into a stationary shock wave (a) moving shock (right facing) (b) stationary shock (right facing) (c) moving shock (left facing) (d) stationary shock (left facing).

2.4.5 Treatment of Boundary Conditions at Duct Exits

At the open end of the two flow channels the flow may be either an inflow or an outflow. Additionally, the flow Mach number at the exit may be either subsonic or supersonic. Therefore, the treatment of each must be accounted for in the analysis. The treatment follows a procedure set forth by Zucrow and Hoffman (Ref. 27).

Consider the unit process for an open end point with outflow at the right hand side of the internal flow field (Fig. 2-9).

The boundary condition at the open end is determined by the external flow field surrounding the exit plane of the duct. For subsonic outflow, the approximation is made that p_4 at the open end is equal to the ambient pressure. Figure 2-9 (a) illustrates the process of an open end with subsonic outflow. If it is assumed that the ambient pressure, p_∞, is known, then the boundary condition imposed on the internal flow field is that $p_4 = p_\infty$. If the details of the external flow field must be considered, then a two- or three-dimensional analysis of the external field must be obtained and the pressure p_4 that the external flow field present to the internal flow field must be used. For all calculations in this research, the jets were assumed to be operating in a static state at known ambient conditions, similar to the experimental data used in the comparison,

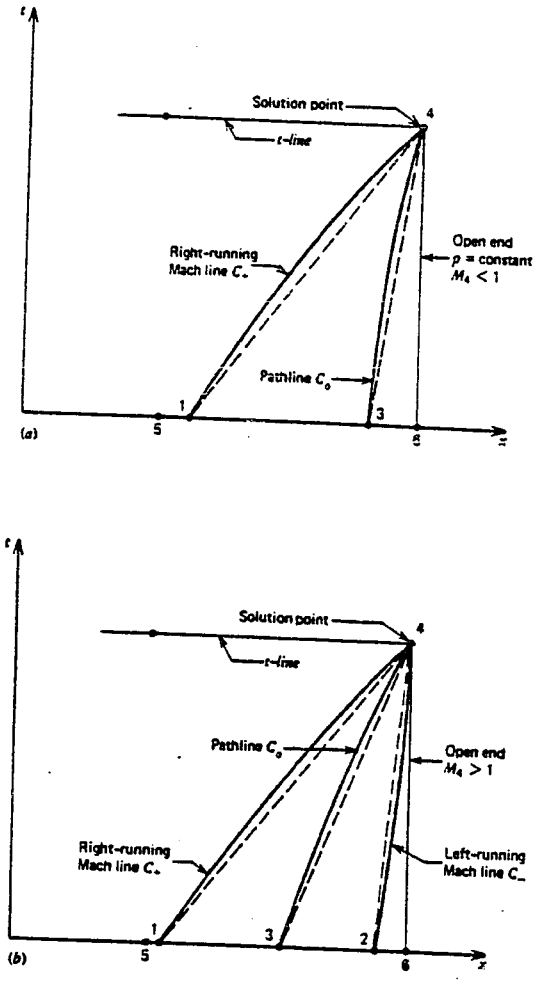

Figure 2-9 Unit Process for Outflow at an Open End
(a) Subsonic outflow (b) Supersonic outflow

and therefore p_4 was assumed to be the ambient value at x_4.

The case for supersonic outflow is shown in Fig. 2-9 (b). For supersonic outflow, all three characteristics originate from within the internal flow field, consequently the flow properties at point 4 are independent of the external flow field. Thus, the basic duct flow analysis is used to determine the flow properties at point 4. While the

foregoing has been developed with a righthanded outflow, an analogous process may be similarly developed for a left-handed flow.

The unit process for inflow is illustrated in Fig. 2-10. The case for subsonic inflow is shown in Fig. 2-10 (a). Note, that only a single characteristic, the right running Mach line C_+, reaches point 4 from within the flow passage. Therefore, two boundary conditions must be specified from the external flow field. As those boundary conditions depend on the particular type of external flow field, the flow was assumed to be static and the ambient pressure and entropy used to establish the flow conditions (Ref. 10).

In the case of supersonic inflow, as illustrated in Fig. 2-10 (b), all three characteristics through the point 4 originate in the external flow field, thus the properties at point 4 are completely determined by the external flow field and are independent of the internal flow field.

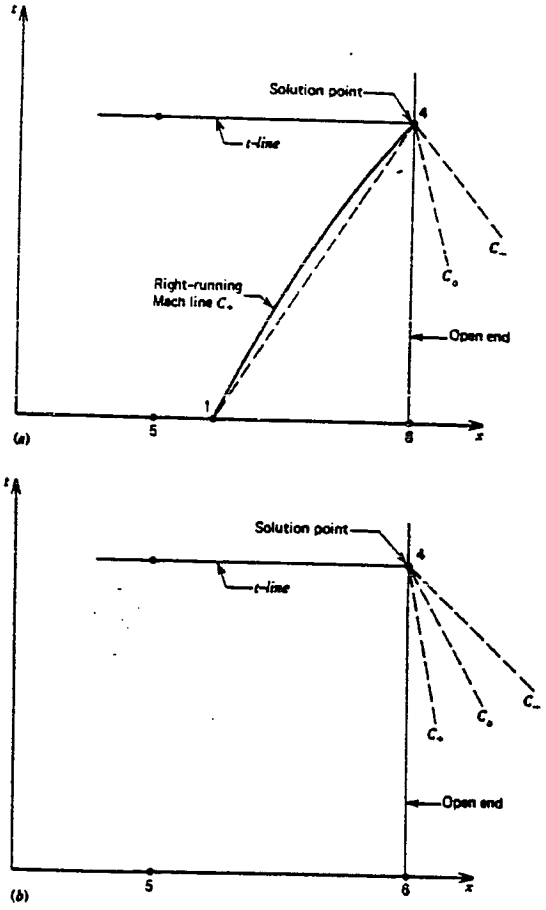

Figure 2-10 Unit Process for Inflow at an Open End
(a) Subsonic inflow (b) Supersonic inflow

CHAPTER 3

PULSATING COMBUSTION MODELING

3.1 The Thermodynamic Limits of the Combustion Process

A combustion chamber is basically a device that is made to convert the chemical energy of two reacting substances into heat. Combustion is, therefore a thermochemical process involving a reaction between two components, that is, the fuel and oxidizer. The fuel is usually the potential source of energy and the oxidizer is the agent that is required to change the chemical species from reactants into products giving off heat. Such a process is known as an exothermic process. Combustion, in its most general sense, is an exothermic process and the products are usually in the form of gases. For air-breathing engines, such as the valveless pulsejet, the oxygen is consumed in the reaction process and the nitrogen acts as a diluent without undergoing any chemical change.

Since the combustion chamber is a system whose primary purpose is the conversion of chemical energy into heat, then it must be designed to satisfy two basic requirements:

1) it must be capable of converting the fuel into heat energy efficiently

2) and should be able to convert the heat energy

into kinetic energy with minimum loss of system energy.

The actual mechanism of combustion is quite complicated and although various theoretical models exist, most results are empirical in nature. However, the elementary processes in the combustion chamber are; the atomization of liquid fuel (usually a hydrocarbon) by the injection nozzle, the vaporization of the liquid droplets by the heat radiated and conducted to them, the preignition reactions between the fuel and oxygen in the air, the ignition and combustion of the mixture, and finally the mixing of the hot combustion products with the excess air.

The purpose of atomization of the liquid fuel is to increase the total surface area of the droplets so that rapid vaporization will be achieved. This is necessary as the required preignition reactions (chaining) are generally carried out in the gaseous phase and are accelerated by the existing conduction of heat in this form. Vaporization and atomization of fuels have been investigated for a large number of industrial applications and a large amount of data exist on these topics (Ref. 22).

Another purpose of the atomization is to decrease the size of the droplets so that they may easily be transported by the airstream. The diffusion of the droplets into the air is via two processes; one, the molecular diffusion, and two, large scale turbulence in the flow field. The former

is so small as to be generally ignored, whereas the turbulent mixing, which is approximately 400,000 times as great, predominates (Ref. 22). Thus the diffusion of the droplets to achieve a uniform air-fuel mixture for combustion via turbulence is of prime importance and has a dramatic effect on the size of combustion chambers which can efficiently be used. But, the generation of turbulence cannot be accomplished without the loss of energy, thus the question to be answered is how to create the turbulent mixing with minimum loss of pressure. As the flame velocity and thus the ignition time are also effected by this turbulent diffusion, the overall efficiency of the combustion process is dramatically effected.

The process of oxidation of hydrocarbon fuels is quite complex. The kinetics of the oxidation mechanism are qualitatively understood and can be broken down into three phases. The first phase is the catalytic oxidation at low temperatures. The second phase is the slow oxidation phase which is very important in that it is directly connected to the ignition lag, or the induction period. The final phase in ignition is inflammation. The ignition lag is a result of the fact that the vaporized fuel must be heated to a temperature to produce the correct chaining combinations for the chemical kinetics to produce the ignition. If sufficient time is not allowed for the preheating and

preignition reactions, ignition will not occur. Thus, with a given combustion chamber design and a given mixture ratio, the time interval for evaporation and slow oxidation can be so reduced by increasing the inlet velocity as to prevent ignition. This is the lean mixture combustion limit. As the mixing of the fuel air stream is not homogeneous, the general result is that only a portion of the mixture can provide combustible material at any time. Since the results depend on the chemical rate process and the theory of turbulent flows and mixing, the present empirical, first order approximations represent the best which presently can be achieved within the limits of the available resources.

The upper limit to the heat which can be added to the system can be approximated by examining the flow in a constant area duct with heat addition, Rayleigh flow. The heating of a subsonic flow will eventually lead to sonic velocity. When this sonic velocity is reached, no further heat addition is possible. In practice, for cylindrical combustion chambers, the limiting fuel/air ratio corresponding to the Rayleigh heat addition limit closely approximates the rich mixture combustion limit. The choking leads to incomplete combustion and eventually extinction.

These limits define the outer operating regions of the combustion process, but do not establish the limits on the

process as it occurs. The major factor affecting the process is that of the velocity of propagation of the flame within the combustor. Normally the velocity of propagation of a flame of combustible gaseous mixture is on the order of a few feet per second. However, under certain conditions, this slow process changes quite suddenly to one of extremely high propagation velocity, on the order of several thousand feet per second. The most basic explanation of this phenomenon was put forward by Chapman (Ref. 32) and Jouquet (Ref. 33). Their approach was to consider a combustion process propagating at a constant velocity through a gas in a duct of constant cross-section. As shearing stresses and body forces were considered negligible, and the process was essentially one-dimensional, this combustion model is normally described as a Rayleigh process. (Fig. 3-1)

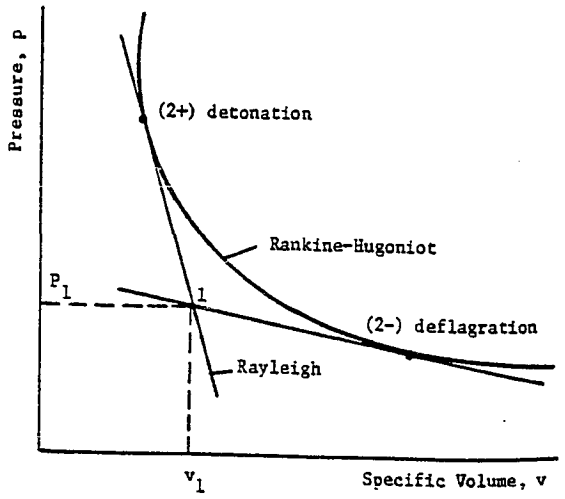

Figure 3-1 Rayleigh flow process

examination of the momentum equation for Rayleigh flow provides a relation between pressure and flow velocity at any station of the region

$$p_i - p = \frac{\dot{m}}{S} (u - u_i) \qquad 3.1\text{-}1$$

(where the subscript i denotes the upstream conditions and s is the cross-sectional area), and the continuity equation, for a cross-sectional area, is given by

$$\frac{u}{u_i} = \frac{v}{v_i} \qquad 3.1\text{-}2$$

Thus

$$\frac{p}{p_i} - 1 = - \frac{u_i^2 S}{p_i v_i S} \frac{v}{v_i} - 1$$

or

$$\frac{p}{p_i} - 1 = - \gamma M_i^2 \frac{v}{v_i} - 1 \qquad 3.1\text{-}3$$

Therefore, the Rayleigh process is always represented in the p,v-plane as a straight line of negative slope:

$$\frac{d(p/p_i)}{d(v/v_i)} = - \gamma M_i^2 \qquad 3.1\text{-}4$$

For a combustion process, M_i is the propagation Mach number

of the combustion front relative to the unburned gas. Therefore, for any Rayleigh process starting at (p_i, v_i), the end point will depend on the amount of total heat added qa, in the combustion process. The completed process must lie on the line given by Eq. 3.1-4, relative to this starting point.

From the first law of thermodynamics (that is conservation of energy), one has

$$dq = c_v\, dT + p\, dv \qquad 3.1\text{-}5$$

or

$$dq = \frac{1}{\gamma-1}\, d(pv) + p\, dv \qquad 3.1\text{-}6$$

As p is a linear function of v, the above integrates to

$$q_a = \frac{1}{\gamma-1}\,(p_f v_f - p_i v_i) + \frac{p_f+p_i}{2}\,(v_f - v_i) \qquad 3.1\text{-}7$$

or

$$\frac{p_f}{p_i} = \frac{\dfrac{\gamma+1}{\gamma-1} + \dfrac{2\,q_a}{p_i v_i} - \dfrac{v_f}{v_i}}{\dfrac{\gamma+1}{\gamma-1}\,\dfrac{v_f}{v_i} - 1} \qquad 3.1\text{-}8$$

(where the subscript f denotes the final condition after

the heat release q_a). This equation is known as the "Hugoniot equation" and as represented in a p, v-plane is called the "Hugoniot curve" for the specific amount of heat released, q_a. The Hugoniot curve is the locus of transformation endpoints for any given initial conditions and for a given value of the heat released. The Hugoniot curve for $q_a = 0$ is called a "Rankine-Hugoniot" curve, in that it represents the locus of end points of adiabatic shock transformations. Therefore, Hugoniot curves for exothermic reactions must be above the Rankine-Hugoniot curve (Fig. 3-2).

Since Rayleigh transformations are physically possible only if the slope is negative (Eq. 3.1-4), the Hugoniot curve is physically significant in two distinct branches, which are separated by a "forbidden region" which covers the entire quadrant in which $dp/dv > 0$.

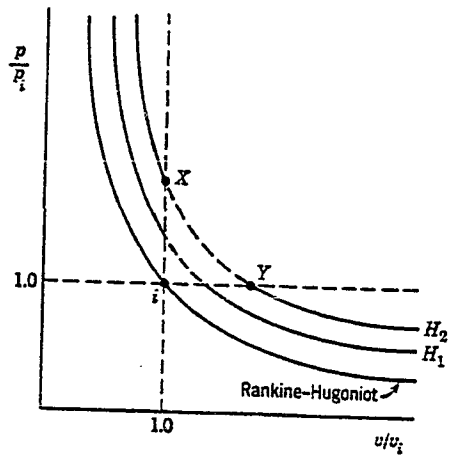

Figure 3-2 Hugoniot curves

By a differentiation of Eq. 3.1-8, the slope of the $[d(^{p}/_{p_i})/d(^{v}/_{v_i})]$ of the Rankine-Hugoniot curve at the initial point is $-\gamma$. Therefore an infinitesimal Rayleigh transformation along the tangent to the Rankine-Hugoniot curve at the initial conditions (p_i, v_i), is itself an infinitesimal isentropic, adiabatic disturbance. Equating Eq. 3.1-4 to the above differential form gives

$$-\gamma M_i^2 = -\gamma \qquad 3.1\text{-}9$$

therefore, it confirms that such disturbances propagate at sonic velocity, that is $M_i = 1.0$.

A combustion process starting at i can only proceed along Rayleigh lines outside the XiY quadrant. The Rayleigh line iY represents a constant-pressure process, with $M_i = 0$, which is a flame at rest with respect to the unburned gas which is practically impossible; and the line iX represents a constant-volume process, in which the flame propagates at an infinite velocity, which is also practically impossible. The slope of the Rayleigh lines below line iY are between 0 and $-\gamma$, therefore the propagation Mach numbers lie between 0 and 1. The slope of the Rayleigh lines to the left of iX are between $-\gamma$ and $-\infty$, which means all the propagation velocities are supersonic. The subsonic processes are called deflagrations and the super-

sonic processes are called detonations.

Examination of the basic Rayleigh process indicates that p will decrease or increase as heat is added depending on the velocity of the propagation. That is $p_f < p_i$ for deflagration and $p_f > p_i$ for a detonation, also one can not have $v_f > v_i$ for deflagration and $v_f < v_i$ for detonation.

A Rayleigh line from the initial condition on a Rankine-Hugoniot curve will intersect the final condition Hugoniot curve at most two points. In the deflagration domain, the intersection nearest the initial point is called the point of "weak deflagration", the other intersection point is called "strong deflagration". Similarly, in the detonation domain, the intersection closest to the initial point is called the point of "weak detonation" and the other "strong detonation". The tangency points are called the "Chapman-Jouquet deflagration" and "Chapman-Jouquet detonation" states, and represent the transformation in which the sonic condition is reached by velocity of the burned gas relative to the transformation front. This is known as the "Chapman-Jouquet condition". In view of the above condition, "strong deflagrations" and "weak detonations" must be eliminated and as can be shown (Ref. 12) are impossible. Therefore, from the initial state, only three essential forms of combustion may occur. They are: one, the "weak deflagration" in which the velocity of the

burned gas is higher than the transformation propagation thus the combustion is a "slow burn" which extinguishes itself; two, a Chapman-Jouquet detonation in which the transformation propagation is equal to the local speed of sound, but, dependent on the local chemical kinetics, may accelerate and become a "strong detonation", or choking may occur which limits the reaction; and three, given the proper preignition conditions, the supersonic ignition or "strong detonation" of the gas.

Once the operation of the physical phenomenon is understood to some degree, limits of performance of the combustion need to be established. This is best realized by first examining the particular type of combustion process one wishes to describe and which basic modeling form best suits the requirements. The latter is left in its detail form until later.

There exist two basic modes of combustion, that is, steady and unsteady. In the steady reaction it is usually sufficient, at first levels of analysis, to assume substantially homogeneous reaction zones or a "volume mode" combustion process. As the effects of friction and area changes can be accounted for in relatively simple models, the average conditions can be simply specified. In the gasdynamic analysis of nonsteady combustion, the transition and placement of the transformation region greatly affects,

and is in turn effected by, the existing chemical kinetics. Therefore, to describe the transport of this region through the unburned gas, the analogy of a "frontal mode" has been developed (Ref. 34)., so that as the reaction transitions from a "frontal mode" or a wave problem to the complete ignition or "volume mode" result, the details may be analyzed.

As the "frontal mode" can be visualized as simply a Rayleigh process, if the front transformations are regarded as quasi-steady, it can be utilized to establish bounds on the performance of combustors in terms of non-steady flows. Beginning with a modified form of Eq. 3.1-3, a generalization may be made, so that linear relations may be analyzed. The relation for the pressure and specific volume

$$\frac{p}{p_i} - 1 = -\upsilon \left(\frac{v}{v_i} - 1\right) \qquad 3.1\text{-}10$$

where the subscript i denotes the initial, unburned conditions and υ is a constant to be determined.

In the Chapman-Jouquet treatment of Rayleigh processes it was noted that the Rayleigh transformation were for $\upsilon = \gamma M_i^2$.

If we define the specific volume variation of a

combustion process as a linear function of time,

$$\frac{v}{v_i} = 1 + k\,t \qquad 3.1\text{-}11$$

where

$$k = (1/t_c)\left(\frac{v_f}{v_i} - 1\right) = \text{constant} \qquad 3.1\text{-}12$$

and t_c is the total combustion time and the subscript f denotes final conditions.

For an approximation to the time history of the release of heat during the transformation, we can use

$$\frac{dq}{dt} = \frac{1}{\gamma-1}(K_1 + K_2 t); \qquad K_1,\ K_2 \text{ constants} \qquad 3.1\text{-}13$$

as suggested by Foa (Ref. 12).

The first law of thermodynamics may be written in the form

$$(\gamma-1)\frac{dq}{dt} = v\frac{dp}{dt} + \gamma\, p\frac{dv}{dt} \qquad 3.1\text{-}14$$

or, in terms of the above variables

$$(1 + k\,t)\frac{dp}{dt} + k\,\gamma\,p = \frac{1}{v_i}(K_1 + K_2 t) \qquad 3.1\text{-}15$$

Integrating yields

$$p = \frac{1}{k\ \gamma\ v_i}\left(K1 - \frac{K_2}{k(\gamma-1)} + \frac{\gamma\ K_2}{(\gamma+1)}\ t\right) + \frac{c}{[v_i(1+k\ t)]^{\gamma}} \qquad 3.1\text{-}16$$

where the constant C can be evaluated at t = o where $p = p_i$

$$c = v_i^{\gamma}\left[p_i - \frac{1}{k\ \gamma\ v_i}\left(K_1 - \frac{K_2}{k(\gamma+1)}\right)\right] \qquad 3.1\text{-}17$$

If C = 0, then p would be a linear function of time

$$p = p_i + \frac{K_2}{k(\gamma+1)v_i}\ t \qquad 3.1\text{-}18$$

If p and v both vary linearly with time, they also vary linearly with one another, therefore for the special case one obtains

$$\frac{p}{p_i} - 1 = \frac{K_2}{k^2(\gamma+1)p_i v_i}\left(\frac{v}{v_i} - 1\right) \qquad 3.1\text{-}19$$

or

$$\upsilon = -\frac{K_2}{k^2(\gamma+1)p_i v_i} \qquad 3.1\text{-}20$$

If $K_2 > 0$, that is the rate of heat release increases with time, then $\gamma < 0$ and the process would lie in the forbidden quadrant of the p,v plane; if $K_2 < 0$, then $\gamma > 0$ and a non-steady explosion will lie in the domain of deflagration or detonation. For the case of a deflagration, if $0 < \upsilon < \gamma$, the path is along the transformation in the p, v-plane of a "weak deflagration". If $\gamma < \upsilon < +\infty$, the path is along the path of a "weak detonation". One should note that the explosion path terminates at the first intersection of the Hugoniot curve corresponding to the heat of the reaction. Once this point is reached, no further reaction can take place as the limit of the heat liberation has been reached.

In the thermodynamic modeling of such processes, as long as the end state is path independent, the selected transformation function for analytical treatments is basically a convenience. A functional representation which has been found to be useful in the generalized study of jet engine performance is the polytropic process.

$$p\, v^n = \text{constant} \qquad 3.1\text{-}21$$

where $n = \text{constant}$

Polytropic explosions have three transformation paths

in common linear explosions, that is, when n = 0, -1, or $\pm\infty$, the polytropic process reduces to a linear process with υ = 0, -1, or $\pm\infty$.

From the first law of thermodynamics, the equation of state for a perfect gas, and the polytropic relation

$$\frac{dp}{p} = - n \frac{dv}{v} \qquad 3.1\text{-}22$$

one obtains

$$dq = \frac{\gamma}{\gamma-1} p\, dv + \frac{1}{\gamma-1} v\, dp \qquad 3.1\text{-}23$$

or

$$dq = \frac{\gamma-n}{\gamma-1} p\, dv \qquad 3.1\text{-}24$$

or

$$dq = - \frac{\gamma-n}{n(\gamma-1)} v\, dp \qquad 3.1\text{-}25$$

If the flow were assumed to be steady and viscous actions neglected, taking the above with the dynamic equation of motion

$$u\, du = - \frac{dp}{\rho} + f_x\, dx \qquad 3.1\text{-}26$$

or

$$d\left(\frac{u^2}{2}\right) = - v\, dp + f_x\, dx \qquad 3.1\text{-}27$$

one gets

$$d\left(\frac{u^2}{2}\right) = \frac{n(\gamma-1)}{\gamma-n}\, dq \qquad 3.1\text{-}28$$

which indicates that the flow velocity always decreases when heat is added in a polytropic process, except in the domain $0 < n < \gamma$, which is the path of weak deflagrations. With all other values of n, the flow velocity decreases if the flow is steady, as heat is added. Therefore the combustion is steady when the value of n is positive and therefore nonsteady when n is negative.

Thus, from the first law and assuming a polytropic process

$$\frac{dv}{v} = - \frac{1}{n-1} \frac{dT}{T} \qquad 3.1\text{-}29$$

and

$$dq = \frac{c_v(n-\gamma)}{n-1}\, dT \qquad 3.1\text{-}30$$

If the subscript i denotes the initial value and f the final value and h the average value, then

$$\frac{T_f}{T_i} = 1 + \frac{n+1}{n-\gamma_h} \frac{q_a}{c_{v_h} T_i} \qquad 3.1\text{-}31$$

and

$$\frac{p_f}{p_i} = \left(\frac{T_f}{T_i}\right)^{\frac{n}{n+1}} \qquad \frac{v_f}{v_i} = \left(\frac{T_f}{T_i}\right)^{-\frac{1}{n-1}} \qquad 3.1\text{-}32$$

The time rate of heat release for polytropic explosion is then given by

$$\frac{dq}{dt} = \frac{\gamma-n}{\gamma-1} k p \qquad 3.1\text{-}33$$

Since $K \neq 0$ depending on whether $n \neq \gamma$, then the time rate of heat release in a polytropic explosion is, at any given pressure, linearly proportional to $|n-\gamma|$.

This demonstrates the analytical limits, in the form of a polytropic process, of the nature of unsteady combustion as it occurs in a valveless pulsejet.

3.2 Present Combustion Modeling

Summary of Present State-of-the-Art Modeling of Combustion Processes

The process of combustion is essentially one in which chemical energy is added to a "system". The chemical energy is then transformed into pressure, which is allowed to expand and perform useful work. In conjunction with valveless pulsejets, the most common form of this addition is in the form of an atomization of a liquid fuel into a combustion chamber which is mixed through turbulent diffusion with the incoming flow. The mixed flow is then ignited and the chemical energy released.

Many models exist which attempt to describe the physical operation of the combustion process, they include zero-, one-, two-, and three-dimensional models as well as combinations of the above. From an engineering viewpoint, the justification of a model is based, to a large degree, upon the following concerns:

a) is it sufficiently accurate

b) how does the method effect the time to obtain a solution

c) how the model may effect the results

Generally, what is needed is an appreciation of the

certain types of models available and their possible applications. As an example, there would be little point in using a complex three-dimensional model for the initial sizing of a combustor. However, it would probably be appropriate to analyze the primary zone conditions and their effects on the wall temperature. Combustion models have been loosely classified (Ref. 35) as 0-, 1-, 2-, and 3-dimensional plus hybrid combinations of the above, and while the classification is not ideal, as some overlapping occurs, it is convenient in terms of ranking the approaches relative to this specific application.

3.2.1 Zero-Dimensional Models

This type of model treats the entire reaction zone as a single unit, and it is typified by the perfectly stirred reaction (or PSR) in which the velocities, temperatures, heat flux densities, and chemical compositions are assumed uniform throughout the reaction zone. An approach to such a system was made by Longwell (Ref. 36) using the well stirred reactor approach. Pressure, temperature, and heat release rates are exponential functions of the concentration, the kinetic rate constant, and the heat of reaction of the fuel and are calibrated via empirical data.

While simple in approach, and thus relatively quick to calculate, the rate equations depend on the homogeneity of

the initial state and are not directly applicable to systems where the mixing processes are predominant.

This model has been used with some success by Kentfield, et al. (Ref. 17), where it is referred to as the "volume mode". The success of this application was dependent chiefly upon the calibration via experimental results and was limited in the analysis to the effects at the throat areas of the combustion chambers on the tuned intake and exhaust channel gasdynamics. Therefore, the results of utilizing such a model are limited in their region of geometric application and depend substantially upon knowledge of the chemical kinetics prior to the analysis.

3.2.2 One-Dimensional Model

Although not as simple as the zero-dimensional models, the one-dimensional models are still relatively simple, and the calculations are only slightly greater than the zero-dimensional model. Beginning with a knowledge of the fluid flow and the chemical heat release, a model may be developed which is no longer mixing limited or reaction limited. The process is similar to the "front mode", as described by Foa (Ref. 12). The assumption is that the combustion takes place at all points of a thin, plane propagating surface. While the actual flame or shock ignition front may be

distorted or broken into a number of surfaces, the macroscopic aspects are amenable to one-dimensional treatment.

The model more closely represents the physical operation of the ignition/combustion process, relative that of a zero-dimensional model and allows for the inclusion of a mixing model of the air stream. In addition, the effects of combustion chamber shaping, combustion position and stability, as well as statistical evaluation of the fuel consumption can be analyzed. The latter is most important in that in zero-dimensional models it is assumed the charge in the combustion chamber is at a stoichometric level and therefore the predictions of fuel consumption are nearly ideal. The model sill requires empirical information as to the heat release rate and additionally the mixing turbulent intensity. The added burden of developing a one-dimensional empirical mixing model yields the distinct advantage of being able to completely analyze the operation of a valveless pulsejet with the same order of model throughout, while maintaining the shortest possible computational time required.

3.2.3 Two-Dimensional Models

As is implied in it title, the two dimensional models employ evaluation of variation in x - y coordinates and are generally suitable for systems where axisymmetric flow pre-

vails. Usually the problem can be simplified if the flow is uni-directional and without circulation (as in ramjets and gas turbine combustors) but in complex flows such as valveless pulsejets, there needs to be adequate modeling of; turbulence, reaction rates, radiation chemical kinetics, and two phase flows. Models have been generated (Ref. 37) in which analysis of jet-engine after-burning "buzz" were successfully investigated using this approach, but computation times for the iterative solutions were orders of magnitude greater than first order modeling.

3.2.4 Three-Dimensional Models

These should be the "all-can-do" models, which if accurate enough, should yield perfect predictions throughout the combustor. Current models predict species, concentrations, temperatures, pressures, and velocities at any point within the combustion chamber. Some models include the prediction of flame radiation and wall temperatures at the price of a more complicated program.

The major problems preventing the general use of such models are:

a) the many assumptions involving flow and turbulence predictions may not be correct

b) reaction kinetics may not be correct

c) effects of carbon formation are not known (this effects the flame radiation predictions)

d) for accuracy of computation, a large number of grid (or mesh) points is required which increases computer time and cost

e) in conjunction with (d), a large computer must be available.

From the above, it can be seen that the chance of developing a satisfactory three-dimensional program is remote.

3.2.5 Hybrid Models

Examination of the above models indicates a need to "cut-and-paste" the applicable portions to the specific problem at hand. The models chosen and their pertinent prediction techniques will depend on the previously mentioned application concerns, that is, accuracy relative to the remainder of the model, computational time and requirements, and the overall effect of the model on the results. Based on the requirements of the analysis of the valveless pulsejet an approach as indicated above was chosen.

3.3 Summary Comparison of Attributes and Deficiencies of Existing Models

Based on the review of the operating cycle of the standard valveless pulsejet in Chapter 2, the following attributes are required of a model for the successful demonstration of the objectives of this research:

i) due to the limited computational resources, the solution time and complexity should be minimized

ii) the model should handle some simplified mixing model to assess the concept

iii) accuracy of approach should be limited to the magnitude established by the gasdynamic analysis of remaining geometry.

Examination of the previously presented models shows that, in the above context, the three- and two-dimensional models greatly increase the complexity of the analytical procedure, by orders of magnitude, in the time and computational resources required and as their details exceed the procedure utilized in the remaining geometry analysis, they were excluded as acceptable in this particular research.

The use of the zero-dimensional, perfectly stirred reactor (also referred to as the "volume model" analysis), has been utilized, as was previously mentioned, successfully in the analysis of the effects of geometric variations of the intake and exhaust geometry, and in this use has

been shown to be adequate (Ref. 17). But, unless taken in a quasi-steady mode, in space and time, the modeling does not allow for the injection and mixing limitations to be accounted for, and while the complexity and computational times are minimum, the ability to evaluate the prime thesis of the research that is that of the Synchronous Injection Ignition concept, is not available.

Examination of the one-dimensional model shows that by use of this concept one can depart from the perfectly stirred reactor to a mixing limited problem. Although not quite as simple as the zero-dimensional model, the simplicity and cost of computation of the one-dimensional model are of the same order of magnitude and are of the same order of accuracy as the remaining geometry analysis. The primary limitation of the one-dimensional model over that of the zero-dimensional model is the estimation and use of empirical mixing and reactions conditions, as the computation of the actual kinetics is nearly impossible due to the nature of the existing knowledge of the combustion process.

In the context of these required attributes and relative model deficiencies, it is apparent that a hybrid model best meets the needs of the present research. The combination of the zero-dimension, perfectly stirred reactor in together with the one-dimensional mixing model allow for the maximum utilization of available resources and would be

within the regime of accuracy desired.

3.4 Hybrid One-dimensional Mixing, Constant Volume Combustion Model

The hybrid combustion model used in this research is a combination of a zero- and one-dimensional combustor models. The combustion process is separated into two distinct operating regions. First, the intake/ignition phase and second, the combustion/exhaust phase.

The intake/ignition phase of the combustion process is the combination of the inflow into the combustion region of the inlet and exhaust ducts of the jet (see Fig. 2-4). The inflow of the intake, when combined with the fuel injection schemes described in Chapter 4, produce the combustion mixture. The ignition of this mixture is then begun by the multiple points of ignition sources present in the inflow of the exhaust duct. The ignition position is established when the exhaust inflow wave intersects the intake fuel air mixture at a point where the mixture is specified.

The combustion/exhaust phase phase is a global, one-dimensional ("control volume" type) analysis to simulate the transient combustion process. The model follows a procedure set forth in Ref. 25, but has been modified for this particular application.

If we split the combustion chamber at the ignition

location and treat each half of the chamber and their adjoining tubes as separate channels, we can assume the ignition location to act as a solid boundary and a control volume for each half of the combustor can be illustrated by Fig.3-3.

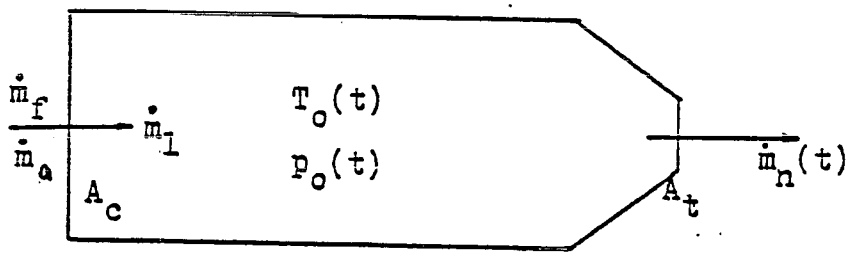

Figure 3-3 Combustion configuration

The control volume equations are the continuity equation

$$\frac{d}{dt}\int_{cv}\rho\, dv + \int_{cs}\rho\, u\cdot n\, dA = 0 \qquad 3.4\text{-}1$$

and the energy equation

$$\frac{d}{dt}\int_{cv} e_i\, \rho\, dv + \int_{cs} h_o\, \rho\, u.n\, dA - \dot{Q}(t) \qquad 3.4\text{-}2$$

These equations can be simplified by assuming the gas to be calorically perfect

$$\begin{aligned} p &= \rho R T \\ e_i &= c_v T \\ h &= c_p T \end{aligned} \qquad 3.4\text{-}3$$

and if the Mach number in the combustor is assumed to be low, the local thermodynamic properties are approximately equal to the stagnation values.

$$p = p_o$$

$$e_i = e_{i_o} \qquad 3.4\text{-}4$$

$$T = T_o$$

To analyze the combustion transient, we will assume the fuel and air mass inflow rates are constant over the short combustion period. We will also assume the outflow to be choked at the combustor nozzle throat during combustion. The validity of this assumption can be rationalized by examining the pressure rise limits and the combustion times of operating devices. For subsonic nozzle flows, this assumption can be replaced by the classical nozzle mass flow equation for unchoked flow (Ref.27). Thus, we will assume

$$\dot{m}_1 = \dot{m}f + \dot{m}_a = \text{constant} \qquad 3.4\text{-}4$$

and

$$\dot{m}_n(t) = \frac{A_t\, p_o(t)}{T_o(t)} \sqrt{\frac{\gamma}{R}} \; \frac{1}{\left(1 + \frac{\gamma-1}{2}\right)^{\frac{\gamma+1}{2(\gamma-1)}}} \qquad 3.4\text{-}5$$

Substitution of equations 3.4-3 through 3.4-5 into 3.4-1 and 3.4-2 and simplifying leads to the following first order, non-linear, ordinary differential equations for the combustion chamber pressure and temperature

$$\frac{dp_o(t)}{dt} = \frac{R}{c_v \tau} \left\{ \dot{Q}(t) - \dot{m}_n(t)\, h_{o_n}(t) + \dot{m}_1 (h_{o_1}) \right\} \quad 3.4\text{-}6$$

$$\frac{dT_o(t)}{dt} = T_o(t) \left\{ \frac{1}{p_o(t)} \frac{dp_o(t)}{dt} - \frac{R\, T_o(t)}{\gamma\, p_o(t)} [\dot{m}_1 - \dot{m}_n(t)] \right\} \quad 3.4\text{-}7$$

These equations, together with equation 3.4-5 for $\dot{m}_n$, can be solved by the Gill method, which is a modified forth order Runge-Kutta method (Ref.26). In equation 3.4-2, $\dot{Q}(t)$ is the heat release rate in the combustor, which is equal to the product of the fuel inflow rate and the enthalpy of the fuel. At steady state

$$\dot{Q}(t) = \Delta H\, \dot{m}_1 (mR) \quad 3.4\text{-}8$$

where mR is the mixture ratio of the inflow at the point of ignition. At the ignition transient, in Fig. 3-4, the burnt gas will include a part of the inflow mixture gas and a part of the original unburned gas in the combustion chamber which is swept by the flame front in a unit time. If one

assumes the burnt fraction of the inflow gas to be proportional to the volume of the burnt gas divided by the whole combustion chamber (control volume), then

$$\dot{Q}(t) = \Delta H \left(\frac{V_f}{XL} FT + \dot{m}_1 (mR) \frac{t}{T_s} \right) \qquad 3.4\text{-}9$$

where V_f is the flame front speed relative to the wall, XL is the length of the combustor, FT is the total fuel mass in the combustor control volume before ignition and Ts is the time period between ignition and flame front impingement on the nozzle wall.

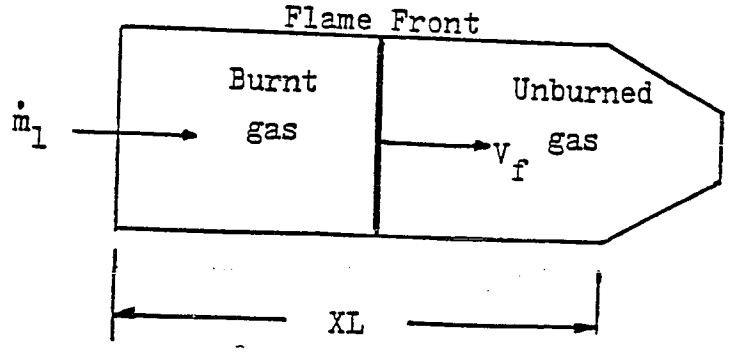

Figure 3-4 Combustion ignition transient

CHAPTER 4

SYNCHRONOUS INJECTION IGNITION

4.1 The Synchronous Injection Ignition Concept

The fundamental objective of this research is the demonstration of the Synchronous Injection Ignition Concept (SII). The Synchronous Injection Ignition concept is that significant improvements in the performance of valveless pulsejets can be achieved via a synchronized, high pressure injection of a metered amount of fuel at the most advantageous point in the operating cycle of the device, instead of the present almost continuous injection of fuel during the whole cycle. The concept is novel in that this research is the first to propose this combination of operational procedures to achieve the indicated performance gains for the valveless pulsejet. The application of high pressure injection of the fuel charge will provide maximum atomization of the fuel, the metering will provide a means of throttling the device as well as provide a form of fuel-air mixture control, and the cyclic control of this injection will insure the maximum combustion efficiency through optimum mixing and ignition timing. The result of this combination of operations will be significant reductions in the specific fuel consumption of the device at thrust levels

identical to conventional valveless pulsejets. The projected magnitude of this increased fuel efficiency would bring the performance of the SII valveless pulsejet, in terms of specific fuel consumption, near that of a conventional turbojet. When combined with the simplicity and cost of the device, relative to the turbojet, the SII valveless pulsejet would provide an attractive alternative to the turbojet in many applications.

4.2 Historical Background

The foundations for the formulation of this concept originate primarily from the work of the French engineers at SNECMA (Ref. 13) and Lockwood at Hiller (Ref. 14) as previously discussed in Chapter 1. The major objective of the French research was to examine the fundamentals of pulsed combustion and to do so they utilized the simplest device then available, the valveless pulsejet. It is in this work that the first descriptions of intermittent fuel injection are discussed. In initial experiments examining the effects of fuel supply pressure on the combustion process, the French experimenters observed the intermittent injection of the fuel when the pressure within the combustion chamber exceeded the fuel supply pressure. It was also observed that the specific fuel consumption of the device decreased with this intermittent injection of the fuel, and

an examination of the contents of the exhaust gases indicated a reduction in the amount of unburned hydrocarbons thus indicating a more efficient combustion process. As the researcher's interest was in pulsed combustion, the majority of this work was presented as improvements in the field of experimental pulsed combustion research rather than improved valveless pulsejet performance.

The researcher primarily responsible for identifying the results of the intermittent injection of fuel on the performance aspects of the valveless pulsejet as well as providing the first systematic study of the effect was Lockwood (Ref. 14). Lockwood's interest was primarily in the performance aspects of the valveless pulsejet and areas of it's possible improvement. His task was the development of the valveless pulsejet into a viable primary propulsion device for vertical takeoff or landing (VTOL) concepts. As one major area of his research, Lockwood examined the effects of intermittent fuel injection on the performance of the valveless pulsejet. Using the French work as a starting point, Lockwood systematically examined the effects of varying fuel supply pressure, fuel mass flow, fuel supply location within the combustion chamber, as well as geometry variations on the performance of the valveless pulsejet. He confirmed the results the French had reported and established limits on the performance of low supply

pressure fuel systems as a means to obtain intermittent injection of the fuel. The majority of these limitations were forced upon Lockwood due to the nature of the applications of the device. Simplicity in construction, operation, and maintenance were paramount, thus schemes utilizing the complex high pressure systems existing at the time of his research limited their application. Lockwood did recognize the importance of maximizing the atomization and mixing for maximum combustion performance and to this end produced the best low pressure systems yet devised, and in his results pointed the way for future research.

Recognition of the inability of low pressure fuel supply systems to provide proper atomization and precise control of the time of fuel addition to the combustion chamber has led to numerous alternate proposals. The majority have centered around the use of some form of pre-injection fuel atomization as in a carburetor. However, the results have been poor. The control of the mixture and the precise timing of the injection during the cycle of the device are almost nonexistent thus efforts in this vein have been discontinued.

The recent technological advances in the microelectronics industry have produced a wide variety of electronic devices which possess the ability to control operations at very high speeds in a precise and dependable manner. The

advent of the microprocessor with its low cost, speed, and ability to be programmed to accomplish complex task has opened new frontiers in the area of process control. Secondary developments in the area of devices to be driven by these microprocessors have include such items as fuel injection systems for automobiles. These items have been developed and proven in everyday use and have opened the possibility of application in other areas. One such area is the SII valveless pulsejet. For the first time in the history of the device the technology exist to precisely control the time, location, and amount of fuel injected into the device with a simple, low cost system. It has been in this context that the present research has been directed. The technology now exist which provides an ability not previously available and allows for a reexamination of the valveless pulsejet technology in terms of these new developments. Thus, this research was an effort to examine the possible improvement to be gained by use of the Synchronous Injection Ignition Concept for the evaluation of possible application of this new technology.

4.3 Modeling of the SII Concept

The principal objective of this research was to evaluate the Synchronous Injection Ignition concept as a means

to significantly improve the performance of the valveless pulsejet and to this end the modeling of that process was of prime importance.

4.3.1 Basic Injection Modeling

The basic model used to simulate the injection of fuel into the air stream included injection location, atomization, mixing, and ignition of the fuel-air mixture as a function of the fuel injection pressure, mass flow within the device, combustion chamber pressure, and wave conditions. The physical location of the injection of the fuel is fixed during the analysis of a particular configuration but can be adjusted from one simulation run to another to allow for the examination of this effect on the performance. Thus, the injection location is an input to the analysis program (described in Chapter 5). The choice of utilizing a fixed input location during the analysis was based on the rationalization that the vast majority of existing applications used a fixed location for the injection and the simulation of these configurations was of primary interest. This choice also allowed for the examination of the effects of various injection locations with a simple change to the input data of the program.

Atomization and mixing of the fuel was simulated via the hybrid model described below. The penetration and

statistical distribution of the fuel droplet size of the injected fuel stream are functions of the fuel supply pressure, the combustion chamber pressure, the angle of the injection relative to the local flow, and the local velocity of the airstream at the injection location of the combustion chamber. The resultant penetration pattern of a transverse injection of the fuel is shown in Fig. 4-1, with the coorelation model used in this study shown in Fig. 4-2 (Ref. 38). In all the analysis performed to date the injection angle has been kept constant at ninety degrees to the local flow to minimize the number of variables. This variable was selected as it appears to carry only a second order effect on the results (Ref. 38). The resultant fuel spray pattern and internal droplet distribution (Fig. 4-3) is then used as a starting point in the analysis of the mixing process of the fuel and air.

The resulting fuel-air mixture is then established along the internal flow path within the combustion chamber with the aid of empirical turbulent mixing coefficients obtained from calibrated models of diffuser flows similar to configurations in this study. The relative internal velocities and flow properties are obtained from the one-dimensional, unsteady, gasdynamics model described in Chapter 2. This then provides the statistical variation of the mixture within the combustion chamber and establishes

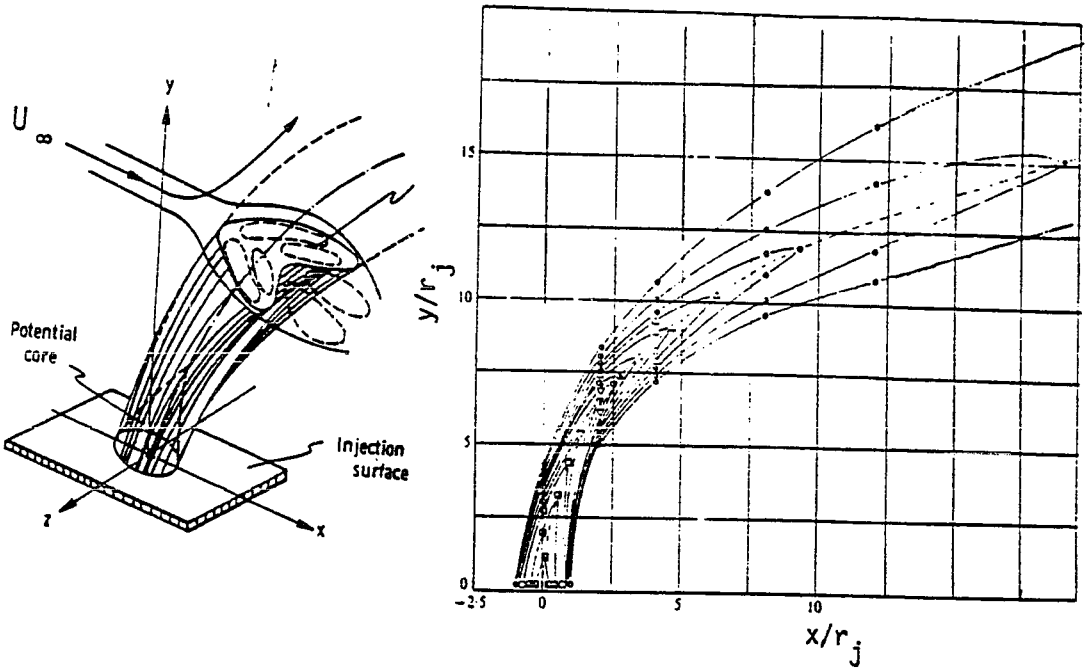

Figure 4-1 Schematic of transverse flow field

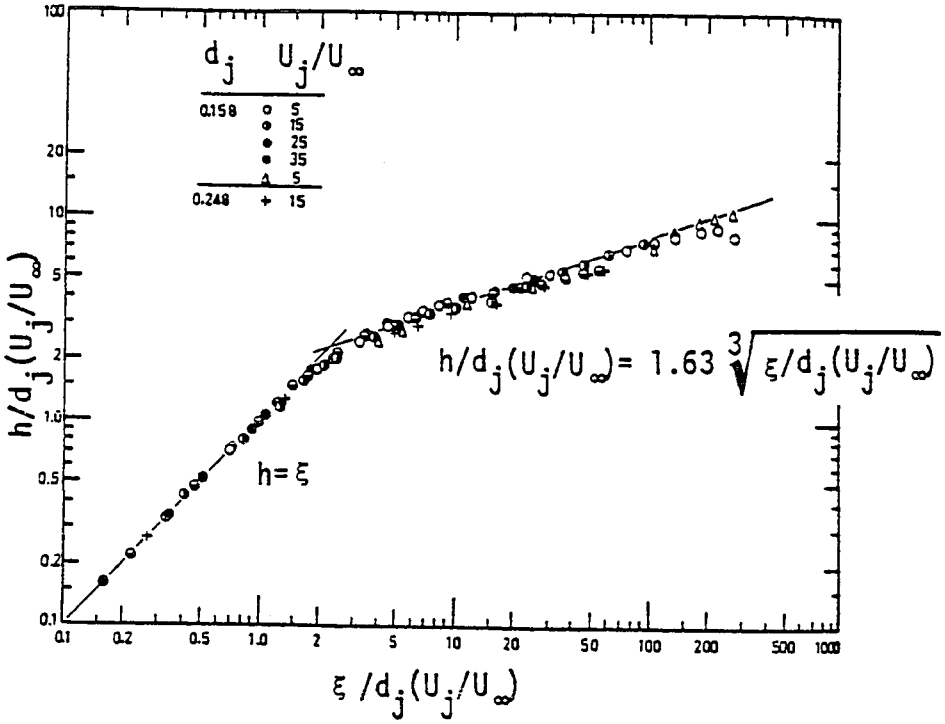

Figure 4.2 Correlation of the trajectory of the jet centerline along the arc length for transverse, h = 90 deg, injection

the ignition and combustion capability of the mixture within the combustion chamber.

The ignition of the mixture is then established by the interaction of the returning combustion products of the previous wave and the mixture at that point where fifty percent of the mixture is at a stoichiometric level. This would be the self ignition case. In the starting case the ignition is assumed to occur at the location of the ignition device, in this case a spark plug. Once ignition was established, the results of the combustion process could be predicted from the mixture information. Thus the combustion efficiency would be a function of the the mixture within the combustion chamber at the time of ignition.

4.3.2 Synchronous Injection Ignition Modeling

The synchronous injection ignition modeling differs from the basic injection modeling in two major areas. First, the amount of fuel injected in the basic injection scheme is a function of the exit area of the injection nozzle and the pressure difference between the fuel supply pressure and the combustion chamber pressure during a cycle of the device. Therefore the flow rate varies during the cycle and so the total amount of fuel injected. In the SII model, the amount of fuel to be injected during a particular cycle is fixed, as is the optimum time of the

injection. Second, the atomization models are somewhat different as the low pressure scheme produces a slightly different statistical distribution than the high pressure scheme. The concentration and percentage of large droplets near the injector is higher for the low pressure scheme, thus the distribution is skewed in that direction.

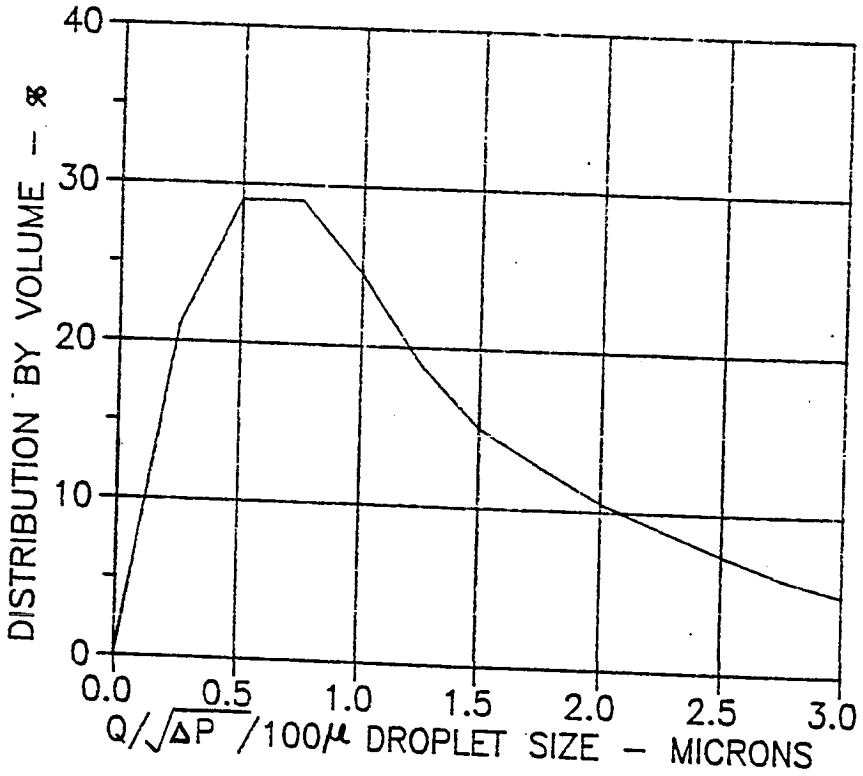

Figure 4-3 Variation of normalized fuel droplet size with fuel rate and feed pressure (Ref. 22)

CHAPTER 5

COMPUTER ANALYSIS

5.1 Overview of Computer Model

A computer program was developed as a part of this research to simulate the unsteady combustion and gasdynamics present in the flow of valveless pulsejets. An existing program (Ref. 29) developed by Wilson and Lee for the transient analysis of MHD channel flows was modified to incorporate multiple channels and a transient combustion model. The unsteady, quasi-one dimensional code employs a real gas method of characteristics analysis, with discrete tracking of shock waves and other discontinuties. Frictional and heat transfer effects, as well as spatially varying cross sectional area are included in the analysis. The combustion transient is based on a hybrid, quasi-one dimensional mixing, constant volume combustion model. The pulsed combustion model incorporates empirical turbulent mixing lengths of the injected fuel and a simple heat release to model the constant volume combustion process.

5.2 Fundamental Analytical Procedure and Program Logic

The analysis of the unsteady operation of a valveless pulsejet, in this program, is separated into three distinct steps (Fig. 5-1). The first of these steps is the analysis of the combustion process. In the initial startup of the pulsejet, the ignition is assumed to take place at the location of the initial ignition source, the spark plug. In the present analysis the location of the spark plug is fixed at the middle of the combustion chamber, half way between the inlet and exhaust channels. Subsequent cycles utilize the ignition location determined from the analysis of the injection, atomization, mixing, and interaction described in previous chapters. Once the location of the ignition has been established, the origin of the coordinate system for the analysis is fixed and the analysis is begun. Note that for a fixed pulsejet geometry, this point will change from cycle to cycle as the mixing properties and ignition vary. This local movement becomes substantial relative to the length of the combustion chamber, moving further and further toward the rear of the combustion chamber as the rich combustion limit is reached. This information is used as an indication of when this limit is reached. The analysis then follows the procedure set forward in Chapter 3, in which the flame front is propagated through the unburned gas from the ignition point toward the

nozzle surface, one ignition wave traveling toward the inlet nozzle and one toward the exit nozzle. This yields the flow properties at the nozzle interface of both the inlet and exhaust channels as a function of time (see Figure 5-1a).

In the second step of the calculation procedure, the above information is then used with the gasdynamic channel flow analysis to predict the flow within the inlet channel and exhaust channels to determine the relative flow conditions through the outflow and reflected inflow portions of the operational cycle (see Figure 5-1b).

The third step in the calculation is the combustion inflow calculation. The results of the inflow portion of the channel analysis provide the flow property variations with time at the nozzle/combustion chamber interfaces. These results are then used to predict the interaction within the combustion chamber of the injected fuel and the turbulent mixing at the inlet and the reignition process due to the interaction of the multiple ignition sources in the returning exhaust wave with the mixture (see Figure 5-1c).

5.3 Program Limitation

The program as it exists is limited due to its development, modeling techniques, and calibration as to the

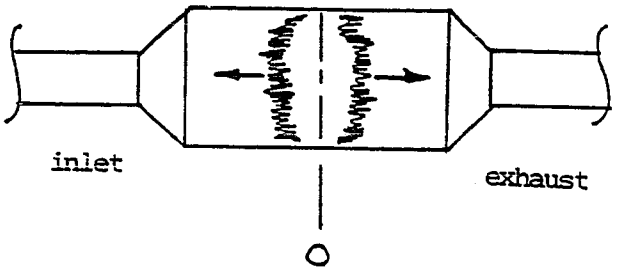

(a) Combstor analysis

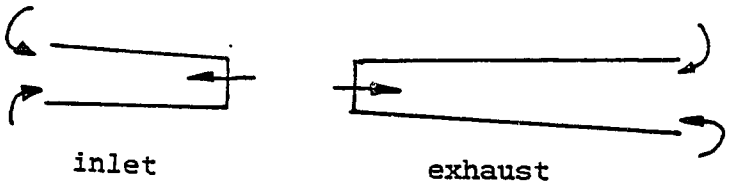

(b) Channel flow analysis

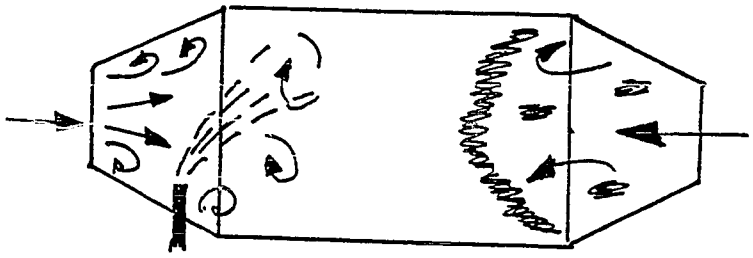

(c) Mixing/ignition analysis

Figure 5-1 Fundamental analytical procedure

geometries and variations it can be used to represent. For example, the simplification to keep the computational times reasonable by use of a one dimensional model of the basic flow, limits the geometric effects one can analyze. Under this restriction, only the area change with distance down the axis of the jet is important, not the shape of that cross section. Therefore in the calibration only valveless pulsejet data of the type represented by cylindrical and conical geometries were used. While it has been shown (Ref. 15) that moderate cross sectional area variations from this will not be affected, it should be noted the analysis was not intended to be, or should be, used for geometries different from the calibrated values. In addition to the above, note that the possible location of fuel injection positions is limited to the region described by the combustion chamber. This limit is somewhat artificial and comes about due to the nature of the three part analysis described above. Although Lockwood (Ref. 14) examined locations within the inlet as possible injection sites and found them to be an advantage for starting, the thrust of this research was in the area of normal operation and therefore no attempt was made to incorporate this flexibility.

Additionally the analysis is limited by the incorporation of a number of empirical relationships in the area of

fuel injection spray distribution, turbulent mixing, and combustion efficiency.

5.4 Computational System and Performance

The code produced for this research was written in ANSI FORTRAN 77 and was compiled on an IBM PC, with a numeric coprocessor, using MicroSoft 3.31 FORTRAN compiler. A complete listing and flow diagram of this program, along with sample results, is included in Reference 39.

The iterative nature of the calculation procedure when combined with the need to examine a number of operating cycles per case limited the number of variations examined. The average time for a steady solution of one cycle, starting as described above, was approximately twenty seven minutes of CPU time. The analysis normally required four to six cycles to reach a stable solution, that is one in which the ignition location had not changed relative to the prior location by more than one-half of one percent of the length of the combustion chamber. If the operation of the pulsejet was near the rich limit, the location became unstable and convergence was not achieved. In cases near this operating region where convergence was achieved, the number of cycles often exceed twenty. Therefore the time to calculate a single data point, such as a specific fuel injection case for a fixed geometry, varied from three to

ten hours of CPU time. The code was modified approximately half way through the study to include a limit on the number of cycles analyzed even if the convergence criteria was not realized. A counter was placed in the convergence loop to stop the process after twenty iterations and an output of the final case calculated produced with a warning message.

CHAPTER 6

COMPUTATIONAL RESULTS

6.1 Introduction

Application of the numerical techniques, developed in chapters 2 and 3, for the performance of valveless pulsejets is evaluated. The effect of heat transfer, friction, unsteady combustion, and fuel injection schemes are considered. The experimental data chosen for the calibration of the numerical analysis is from Lockwood (Ref. 40). The configuration selected for the calibration was the HH-1M valveless pulsejet illustrated in figure 6-1. The rational for the selection of this configuration and data set were; one, the data set is the most complete available in the literature at this time, and second, the HH-1M represented

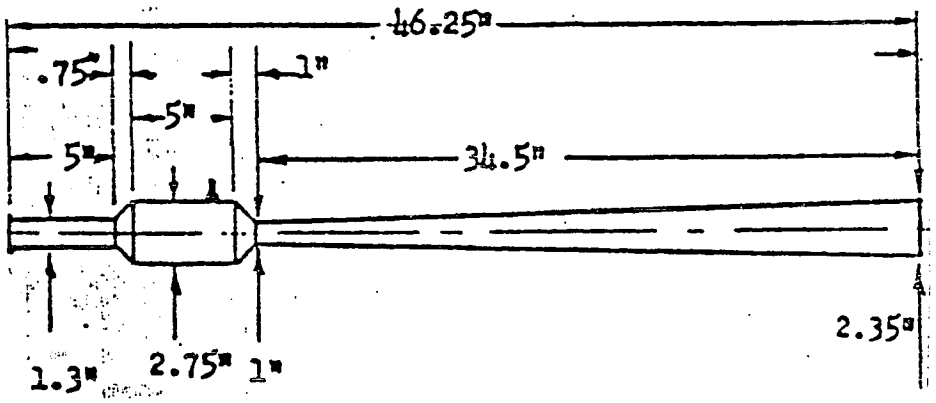

Figure 6-1 Geometry of the HH-1M Pulsejet

the most optimum geometry, in terms of performance, of the series of configurations examined.

As an apriori knowledge of the quantitative effect of each of the parameters listed above was not available, the analysis was initially begun by ignoring the effects of heat transfer and friction. These effects were subsequently added, in turn, until a full performance evaluation could be made. By use of this procedure, the separate influences of the individual parameters could be quantified. The results of the complete model were then compared to the known performance of the HH-1m unit. A calibrated prediction model was then generated by adjusting the ignition sequencing (that is, the relative mixture ratio at the point of ignition) and the initial flame front velocity at the ignition until the combustion chamber pressure variation with time was simulated.

Performance predictions of the calibrated model were then compared with results from a series of geometries for which experimental data were available. The comparison of these different geometries and experimental data bases were made to determine the applicability of the calibrated model for general use.

Finally, a comparison of the two fuel injection schemes was made, using a fixed geometry, to evaluate the relative performance and establish the feasibility of the

Synchronous Injection Ignition concept.

6.2 Calibration of Model with HH-1M

The geometric location and numbering of the stations of interest is presented in figure 6-2. Station 1 is at the exit plane of the inlet channel. Station 2 is at the inlet /combustion chamber interface plane, or the inlet nozzle plane. Station 3 is the combustion chamber/exhaust interface, or the exhaust nozzle. Station 4 is the exit plane of the exhaust. Finally, station 5 is the mid combustion chamber plane. These station numbers are used as a

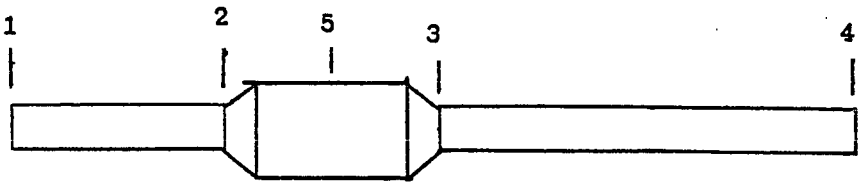

Figure 6-2 Jet station numbering

subscript on the appropriate non-dimensional time, velocity, and pressure terms. As stated, the time, velocity, and pressure terms are presented in a non-dimensional format. This was done to clarify the presentation of the results and allow for the comparison of jets of various sizes and operating conditions. The normalizing constants are; for

the time, the time of one cycle, for the velocity, the ambient stagnation speed of sound, and for the pressure, the ambient static pressure which was assumed to be the stagnation pressure. All calculations were made at standard sea level conditions, thus P_{amb} = 2116.2 lb/ft^2 and a_o = 1117 ft/sec.

6.2.1 Calibration of the Combustion Model

Initial runs of the program indicated a problem in defining the termination of one cycle and the beginning of the next. For a fixed geometry and operating condition, the cycle time varied as much as eight percent from one calculation to the next. The difficulty was traced to the original definition of the termination of the cycle. that is, when the net mass inflow into the combustion chamber was zero. A combination of error in the tracking of the temperature and pressures affected the mass flow calculations. The problem could have been eliminated by the selection of a finer grid in the numerical procedure, however this could only be accomplished at a substantial increase in the computational times. The solution was to terminate the cycle when the net mass inflow into the combustion chamber, across stations 2 and 3, changed from positive to negative (Ref.18).

Based on the combustion geometry illustrated in figure

6-1 and the experimental combustion chamber pressure rise with time in figure 6-3, the values of the ignition sequencing and the flame front velocity were varied to produce the best simulation. Initial values of fifty percent mixture ratio for the ignition sequencing and flame front ignition velocity of three hundred meters per second (Ref. 6) were used with perturbations up to plus and minus fifty percent of these base values. Examination of figure 6-3 revels the following: (Note the non-dimensional time in this figure is based on the experimentally measured rise time of the pressure from ambient to peak chamber value.) one, the principle effects of the variation of the ignition sequencing are in the correlation of the predicted verses the measured location in time of the peak pressure and in the value of the peak, and second, the primary effect of the ignition velocity is on the time of combustion and thus the peak value, with a secondary effect on the time location of the peak. Based on these results a maximum correlation of the experimental curve was achieved with a sixty percent mixture ratio at ignition and an ignition flame velocity of approximately four hundred meters per second, which corresponds favorably with previously obtained values (Ref. 6).

These adjusted values were then used in all other calculations of combustion chamber performance. While these

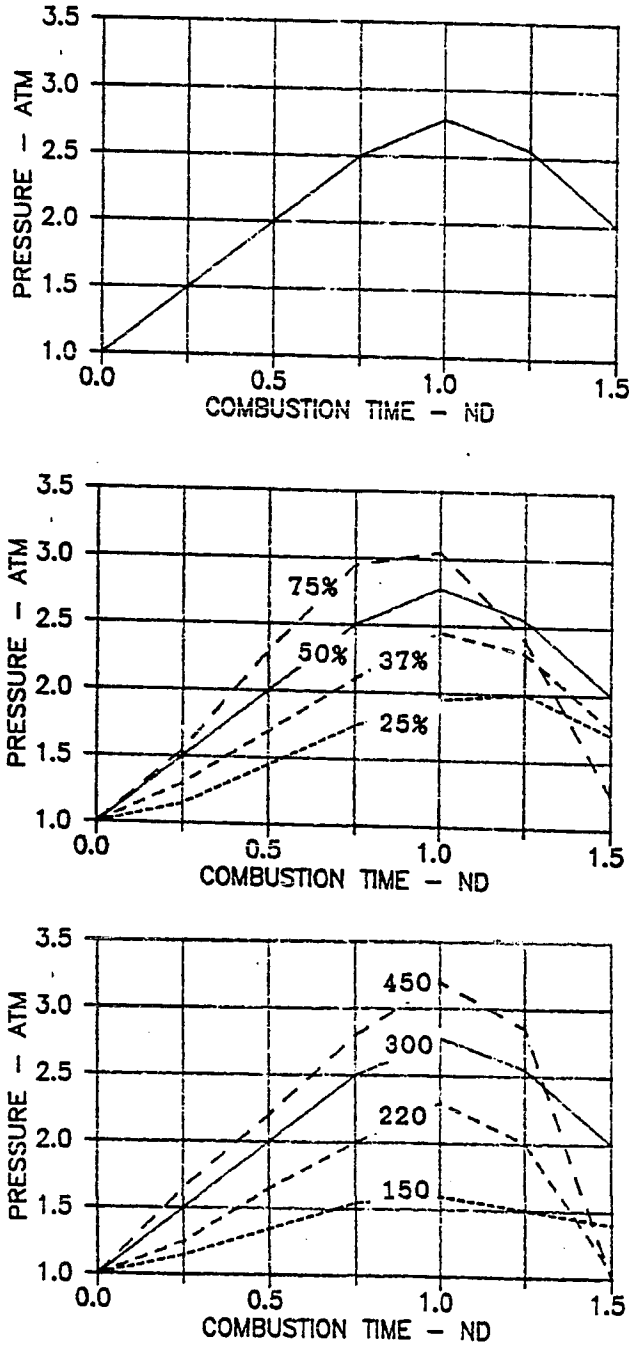

Figure 6-3 Combustion chamber peak pressure variation of HH-1M at 26 lb_f/hr fuel flow rate
(a) Experimentally measured pressure
(b) Variation of ignition sequencing
(c) Variation of ignition velocity

correlation values will vary slightly with combustor geometry, they will remain valid for the geometries evaluated (Refs. 40,16,13).

6.2.2 Correlation of Combustion Chamber Pressure Time History

Experimental time histories of the combustion chamber pressure at station 5 are presented in figure 6-4 for two different operating conditions. The corresponding predicted time histories of the pressure agree fairly well with the experimental values. The two conditions evaluated were at approximately forty percent fuel flow and eighty percent fuel flow to evaluate the effect of different operating conditions. The model prediction appears to be more accurate at the high fuel flow rate condition. This is probably a result of the fact the calibration was performed at the higher flow rate condition.

To evaluate separately the effects of both the wall heat transfer and the wall skin friction, the program was modified to utilize an input value of the Stanton number instead of the Reynolds analogy form in equation 2.4.1-9. Thus, the quantitative nature of the two effects on the prediction model could be evaluated.

6.2.3 Evaluation of Heat Transfer and Friction Effects

The values of the pressure, velocity, and temperature for the station of interest are shown in figure 6-5 for the baseline geometry of figure 6-1, with no friction or heat transfer. The values shown are for the 12.5 lb_f/hr fuel flow point.

The lack of frictional effects on the predicted values of the model resulted in dramatic increases of the thrust after the fifth cycle due to supersonic flow in the exhaust. Additionally, the model predicted fully cyclic operation only after ten cycle calculations. Thus, when compared with the case with friction, where cyclic operation was achieved within four to six cycles, the friction proved to have a damping effect and actually decreased the computational time required to achieve a solution.

The model was then rerun including the effects of wall heat transfer but no wall skin friction. Selection of a Stanton number was based on previous evaluations (Ref. 18) and was selected to be 0.0012 for the best correlation. Figure 6-6 shows the normalized pressures, velocities, and temperatures for this case. Comparison of figures 6-5 and 6-6 indicate no significant changes, however the thrust decreased approximately six percent.

Finally, the model was run using the calculated wall skin friction and the Stanton number as discussed in

chapter 2. The results are presented in figure 6-7.

Considerable changes occurred with the inclusion of the friction effects. The non-dimensional velocities U_3 and U_4 were significantly reduced. There was also a slight reduction in the value of the peak pressure achieved, and the overall thrust decreased by approximately twenty two percent.

The reduction in exhaust velocity also changed the ratio of the exhaust thrust relative to the inlet thrust. Comparison with the results of reference 14 indicate the ratios, as adjusted by the inclusion of the friction, closely correlate with experimental values. The numerical model was also found to achieve cyclic operation by the forth or fifth cycle.

6.3 Comparison of the Model with Experimental Results

The calibrated numerical model was exercised over a range of pulsejet sizes and combustion chamber geometries to determine the effects, if any, of the discrete calibration. Geometries were chosen which corresponded to configurations for which experimental data existed. The only limiting criteria was the combustion chamber be developed from conical sections, as cross sectional area shape changes had been shown to have some effect. The underlying reason for

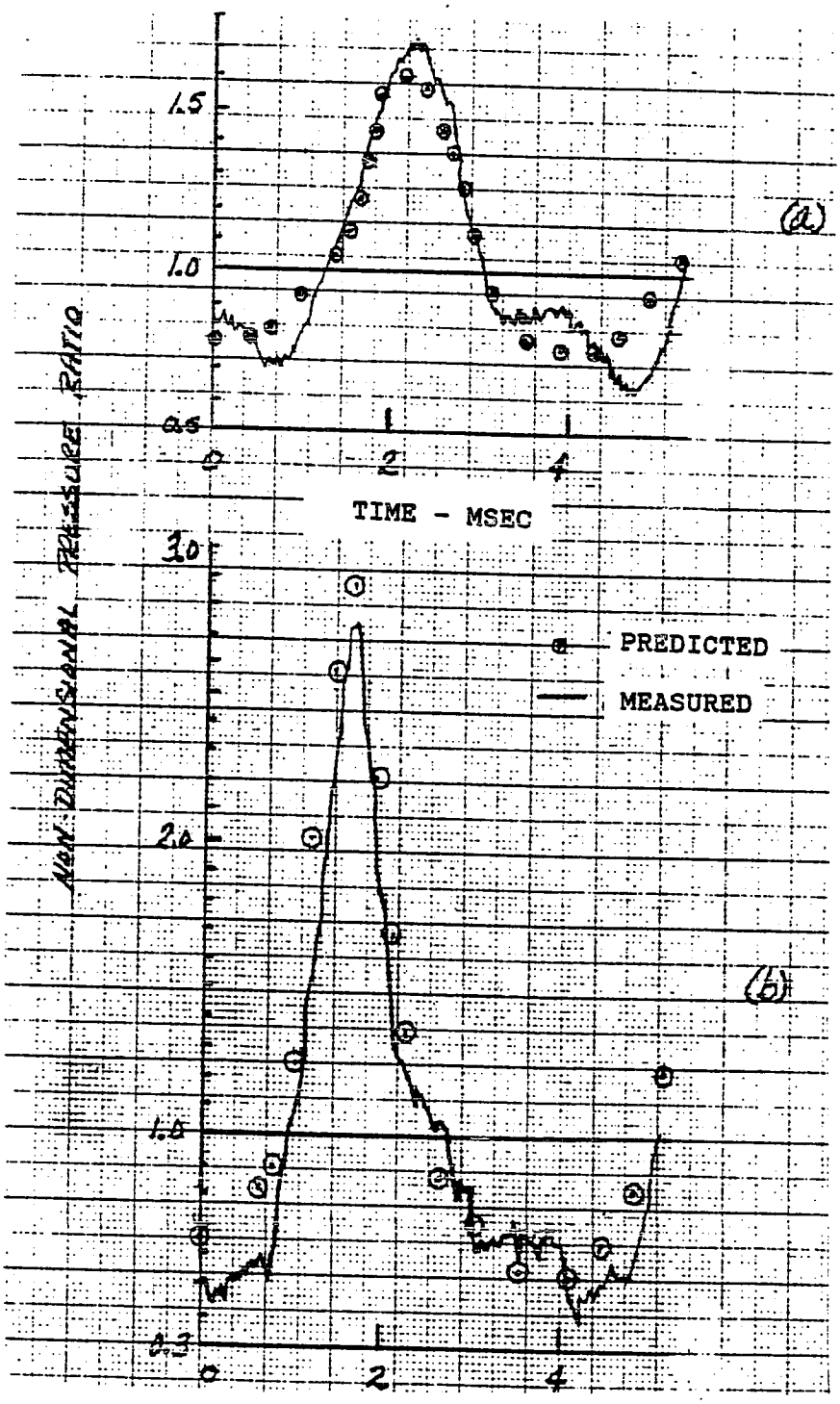

Figure 6-4 Comparison of predicted and experimental combustion chamber pressure with time of the HH-1M valveless pulsejet
(a) 12.5 lb_f/hr (b) 26 lb_f/hr

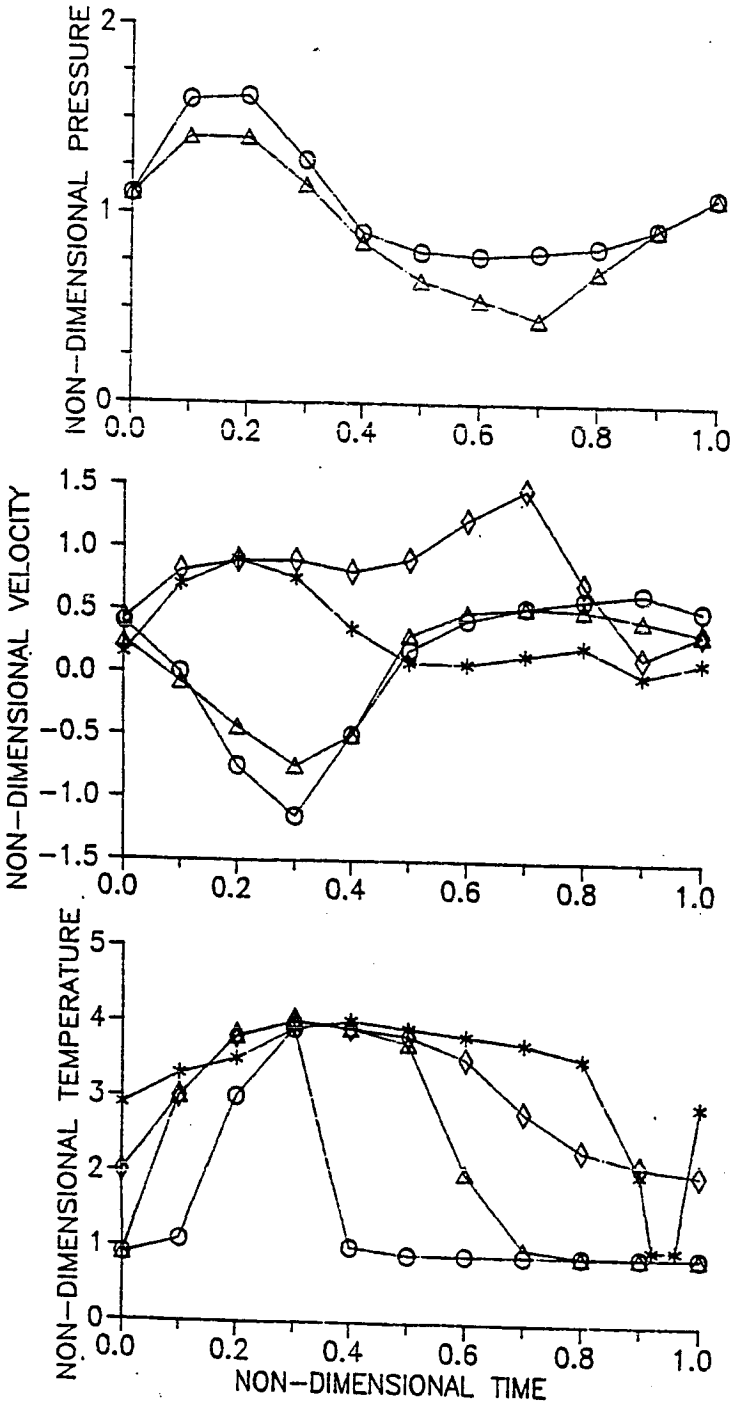

Figure 6-5 Pressure, velocity, and temperature variations in the HH-1M at the fifth cycle with no friction or heat transfer
(a) Pressure (b) Velocity (c) Temperature

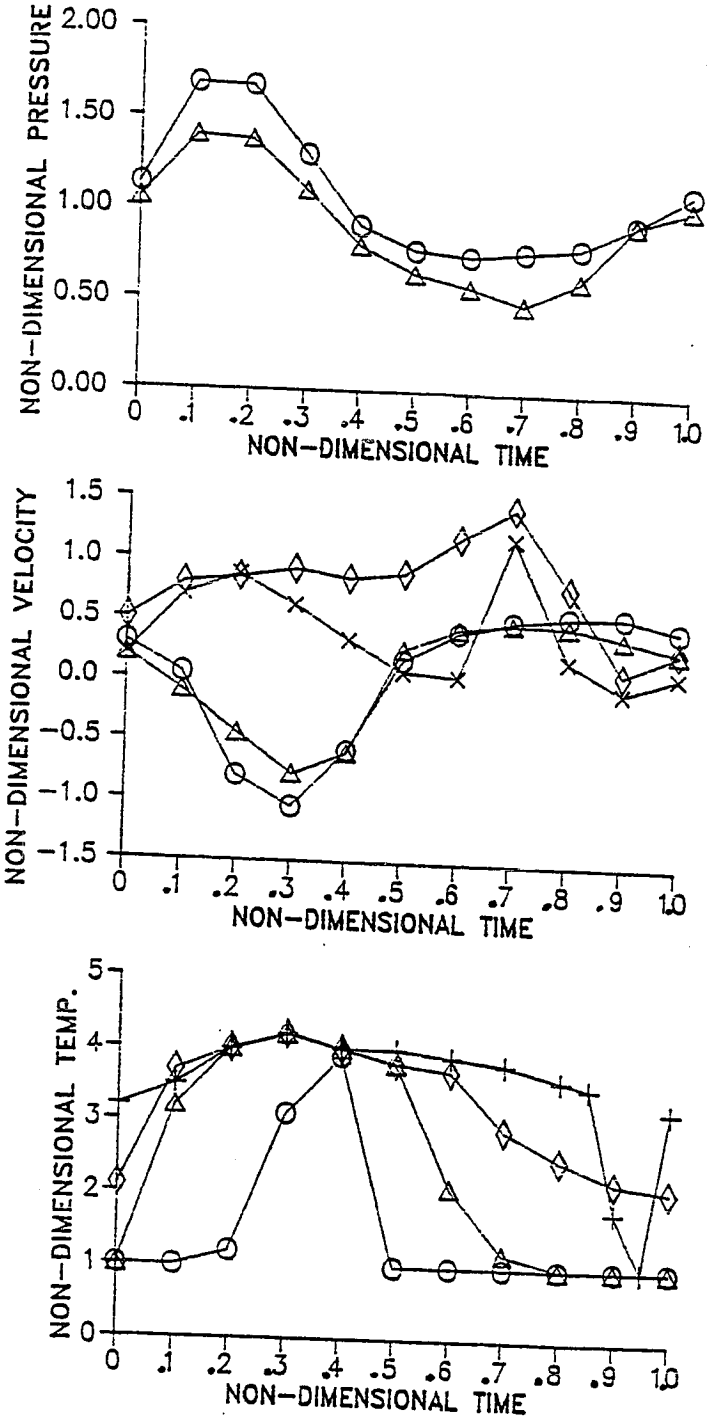

Figure 6-6 Pressure, velocity, and temperature variations in the HH-1M at the fifth cycle with no friction but with heat transfer
(a) Pressure (b) Velocity (c) Temperature

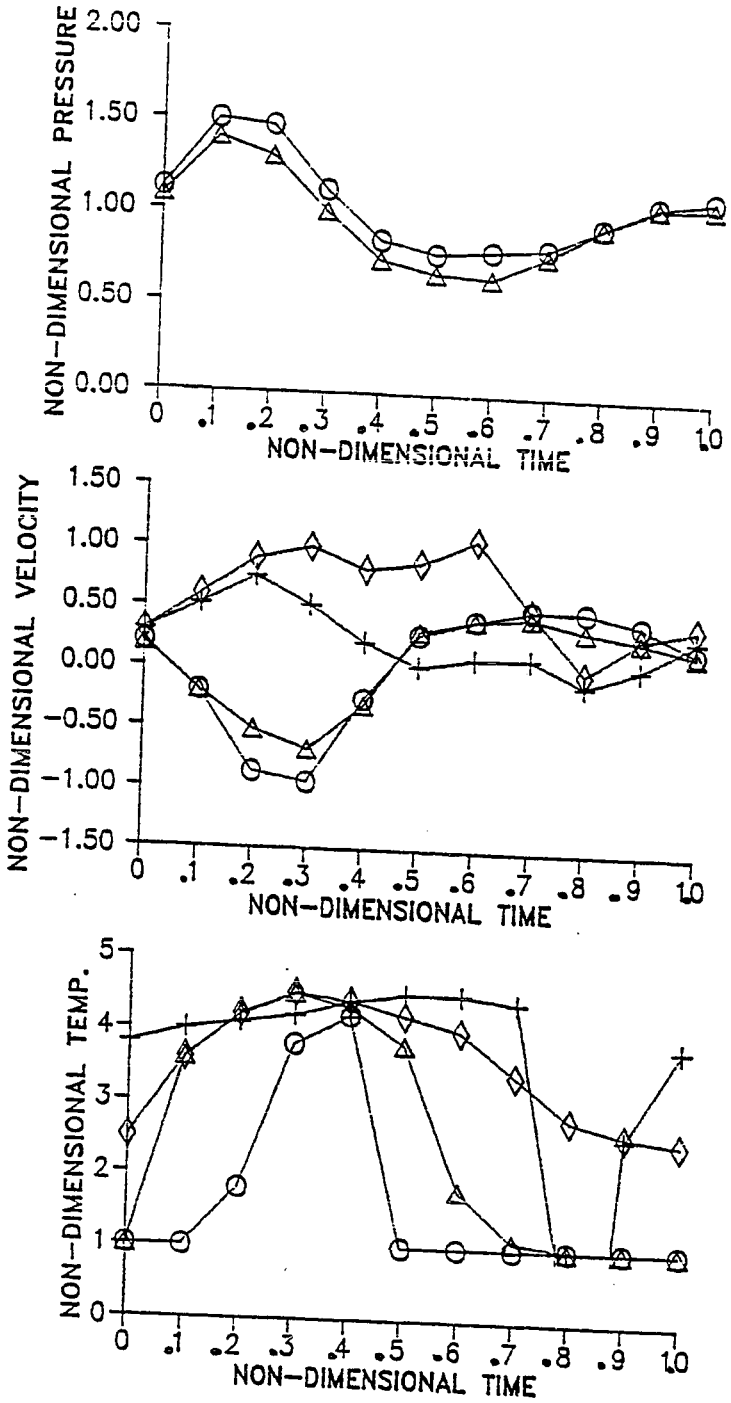

Figure 6-7 Pressure, velocity, and temperature variations in the HH-1M at the fifth cycle with friction and heat transfer
(a) Pressure (b) Velocity (c) Temperature

this evaluation was to insure the ability of the numerical model to accurately simulate other geometries and thus insure the viability and feasibility of the numerical model as an engineering design tool.

The pulsejet configurations selected for this evaluation included the HH-1M for which the original calibration was performed (Fig. 6-1), the Saunders-Roe 5.4" valveless pulsejet, and the SNECMA Ecrevisse (Fig. 1-12). The primary difference in these jets is in the diameter of the combustion chamber and the inlet diffuser cone geometry.

The basic performance of each of the above pulsejets is shown in figures 6-9,6-10,and 6-11. Note that in each case the predicted values are in good agreement with the published experimental values. The only discrepancy appears in the region of high fuel flow rates. The prediction model appears to be slightly optimistic in terms of the basic performance predictors. This optimism appears to be due to the fact the fuel feed orifice was assumed to be constant geometry and the fuel rate was adjusted by adjusting the feed pressure. However, in all three configurations the fuel feed nozzles were of the impact type and thus as the rate and pressure increased the orifice gap increased (Ref. 40). Additionally, as the combustor size is decreased the variations are larger. These are assumed to be due to the smaller mixing length times and diffuser performance.

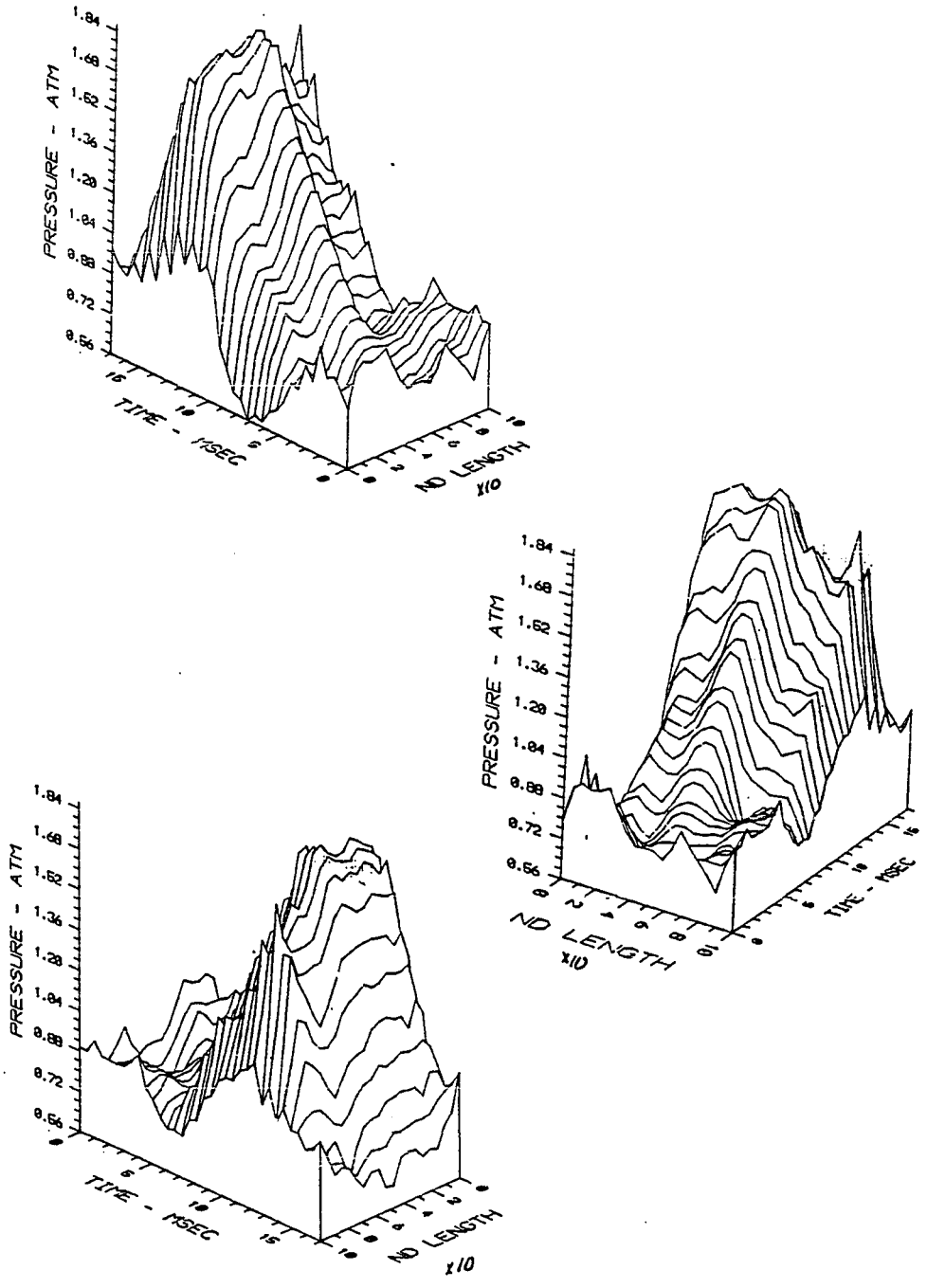

Figure 6-8 Time history of pressure along the axis of the HH-1M

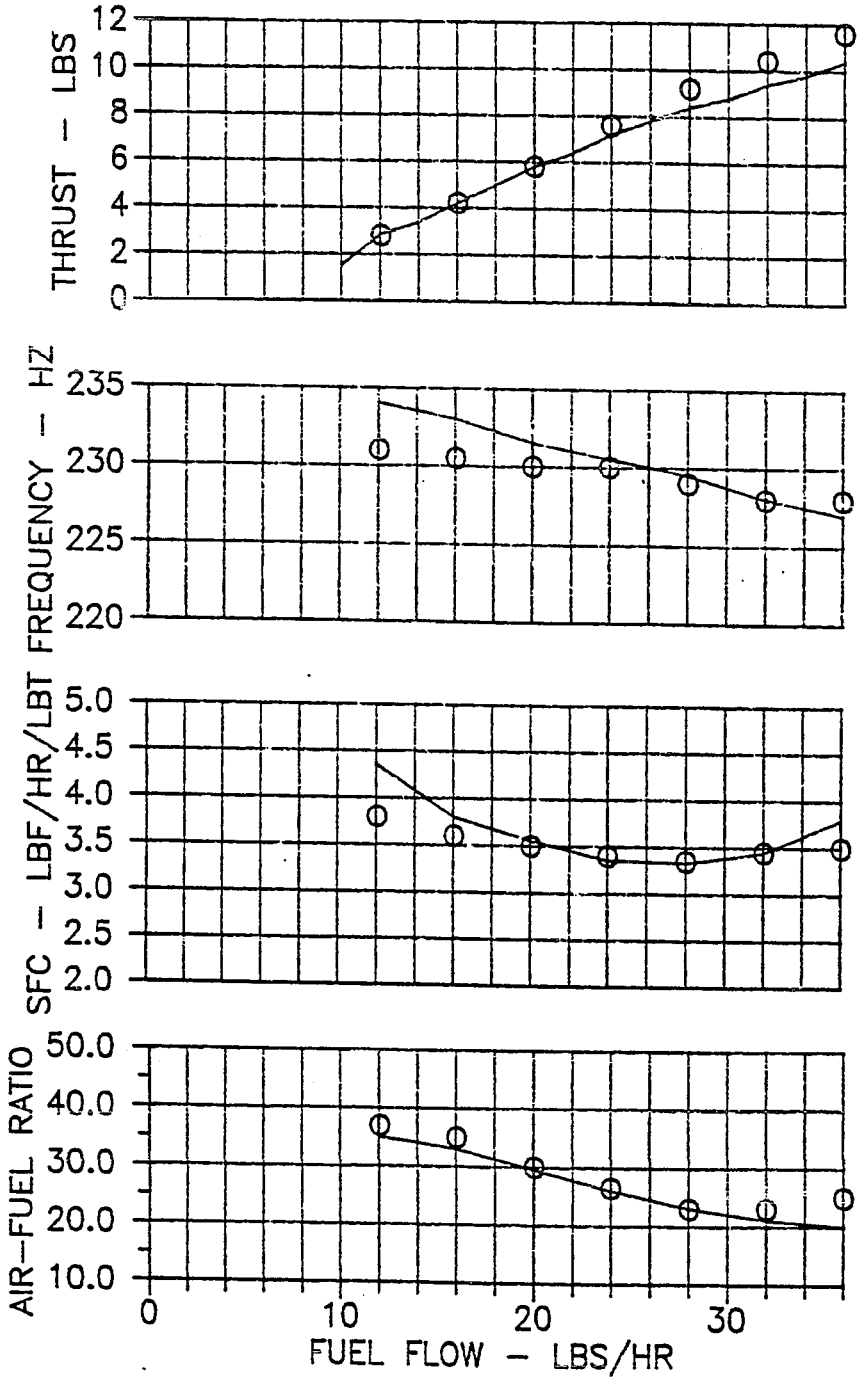

Figure 6-9 Comparison of predicted and measured performance of the HH-1M valveless pulsejet

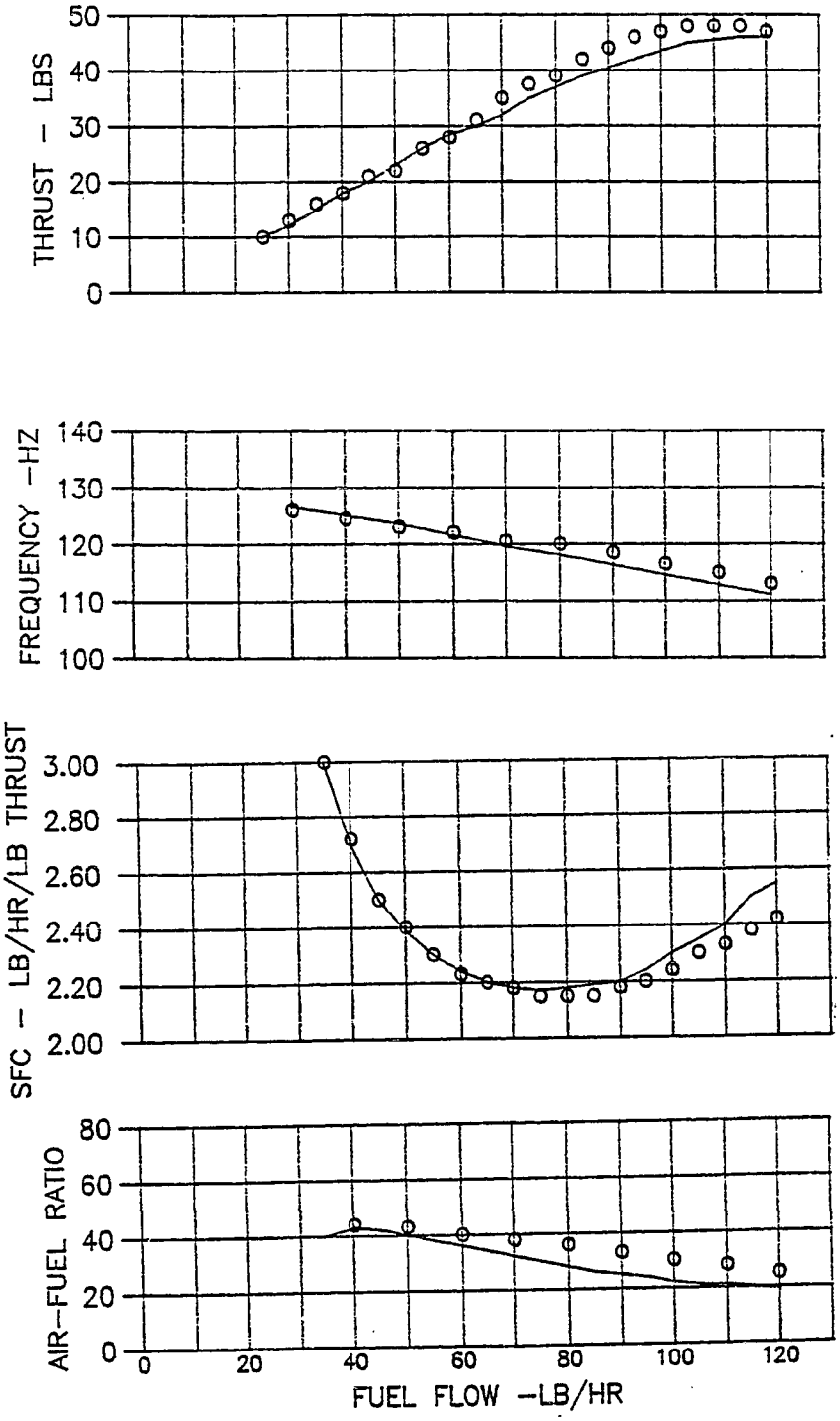

Figure 6-10 Comparison of predicted and measured performance of a 5.5 inch valveless pulsejet

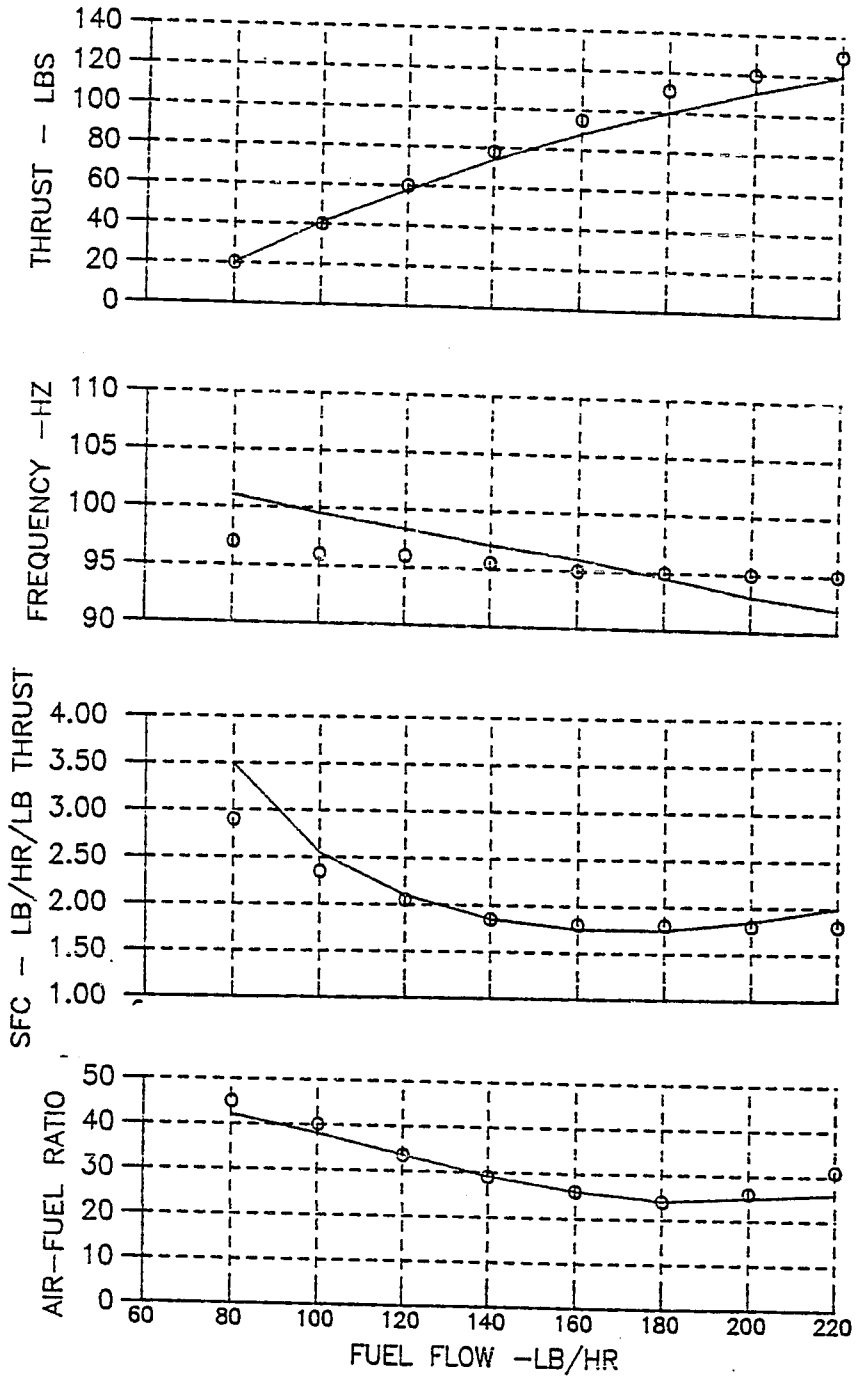

Figure 6-11 Comparison of predicted and measured performance of a 6.9 inch valveless pulsejet

Decreases in chamber size are accompanied by reduced diffuser turbulent mixing and thus reduced combustion efficiency. However, the results confirm the applicability of the numerical procedure as a design tool.

6.4 Comparison of Intermittent, Low Pressure Injection and the Synchronous Injection Ignition Scheme

As stated in chapter one of this report, the primary objective of this research was to evaluate the performance capability of the Synchronous Injection Ignition concept as a means to significantly reduce the specific fuel consumption of a standard valveless pulsejet. This was accomplished by evaluating the the two fuel injection schemes for a given geometry with the calibrated model. The configuration selected for this evaluation was the Saunders-Roe 5.4" diameter valveless pulsejet (Ref.16). The selection of this configuration was based on the following; first, the basic size of the device removes it from the range of concern due to variations in the performance of the diffuser; second, a complete set of performance data was available for numeric model verification; third, the injection position was fixed (unlike the HH-1M, which varied depending on the test); and fourth, the comparison between the numeric model and the experimental results in the previous evaluation were one of the better correlations.

The results of the comparison between the two injection schemes can be seen in figure 6-12. The lower fuel rate scale is expanded relative to Figure 6-10 to accomadate the Synchronous Injection Ignition concept. Note the radical difference in the specific fuel consumption and the air-fuel ratio. The minimum value of the specific fuel consumption for the Synchronous Injection Ignition scheme is approximately half that of the low pressure, intermittent injection scheme. The vast majority of this difference can be seen in the air-fuel ratio difference. Approximately ninety percent of the specific fuel consumption improvement is due to the increase in the fuel-air ratio The remaining ten percent appears to be due to increased combustion efficiency, which can be seen from the minor increase in thrust and operating frequency. The table below gives a summary comparison of the performance values at a thrust of 35 pounds, which is near the minimum specific fuel consumption point for this configuration.

This evaluation demonstrates the capability of the Synchronous Injection Ignition concept as a viable means to significantly reduce the specific fuel consumption of the standard valveless pulsejet. To better understand how this improvement comes about one needs to examine the factors in the injection scheme which contribute to these performance differences.

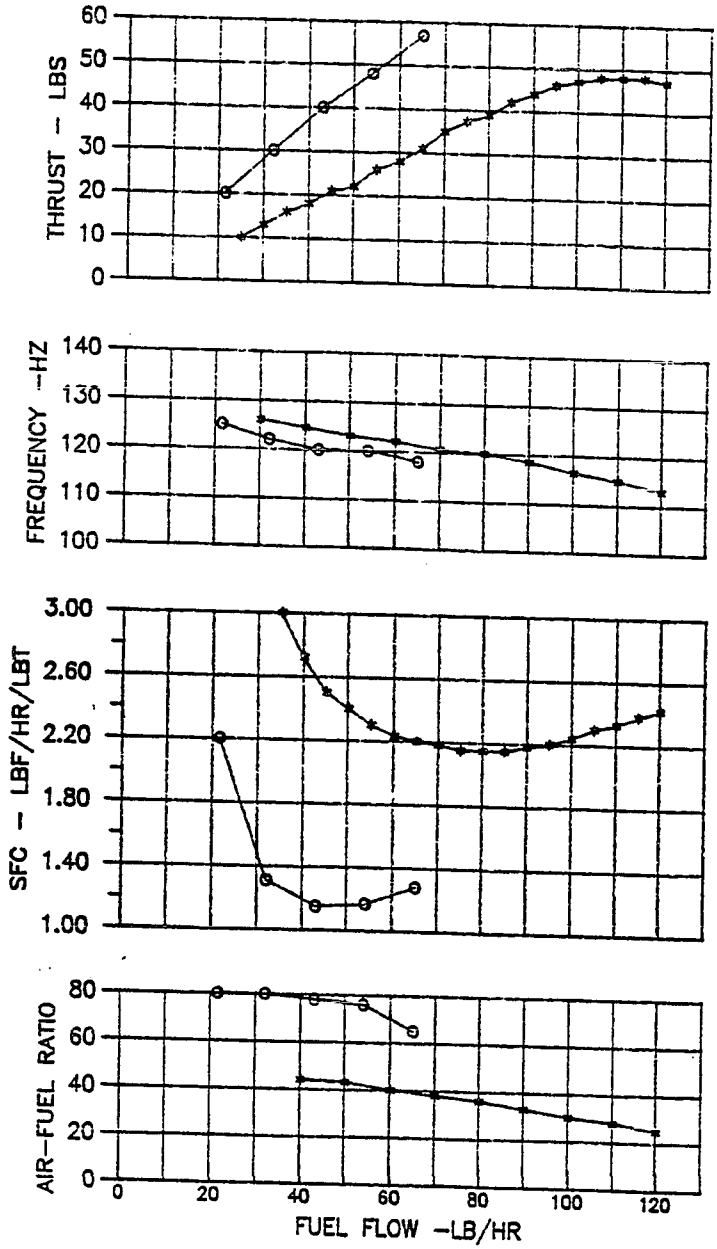

Figure 6-12 Comparison of low pressure, intermittent injection with synchronous injection for the Saunders-Roe 5.4 Inch Valveless Pulsejet

COMPARISON OF RELATIVE PERFORMANCE OF THE TWO INJECTION SCHEMES TO IDEAL FOR THE SAUNDERS-ROE 5.4 INCH VALVELESS PULSEJET

		STANDARD	SII	IDEAL
Thrust	(lb_f)	35	35	35
Air-fuel ratio	(-)	29.4	63.0	71.0
Specific fuel consumption	($lb_m/hr/lb_f$)	2.17	1.18	1.05
Fuel flow	(lb_m/hr)	75	41	36

The fuel injection schemes are discussed in chapter 4. The non-dimensional variation of the pressure within the pulsejet at the injection location is shown in figure 6-13. The solid line represents a 3 psig low pressure feed system. As one can see the fuel feed pressure exceeds the combustion pressure for approximately sixty-five percent of the cycle time (0.6 to 0.95). To use a lower pressure in an attempt to minimize this time period results in a lower pressure difference and thus a larger average drop size and poorer penetration of the fuel spray and thus reduced mixing and combustion efficiency. Thus, the combustion efficiency falls more rapidly than the fuel flow reduction at lower pressures. The above overpressure was experimentally determined (Ref. 40) to be the optimum for low

pressure schemes.

For the fixed fuel feed orifice, the fuel flow rate will be proportional to the difference in the chamber pressure and the feed pressure with time. This variation is illustrated in figure 6-14.

Three major factors affecting the performance of the low pressure, intermittent injection scheme relative to the synchronous injection are; one, the mean droplet size due the magnitude of the difference in the injection pressure difference and the actual fuel flow rate; two, the relative penetration and mixing of the fuel spray pattern; and three, the relative location in time within the cycle of the peak flow rate. The combination of these effect the mixture ratio and ignition delay and ultimately lower the combustion efficiency. To evaluate the effect of the injection rate timing, one needs to examine both figures 6-13 and 6-14. Note that the fuel flow rate (which is proportional to the feed pressure difference) peaks near the non-dimensional cycle time of 0.2 for the low pressure, intermittent injection scheme. Examination of the non-dimensional pressure value at this same time in the pressure-time curve indicates the pressure is at an inflection point and is at a minimum. This point corresponds to a near zero velocity at station 2 (the inlet nozzle, figure 6-7b). Thus, the maximum fuel flow rate occurs when the velocity

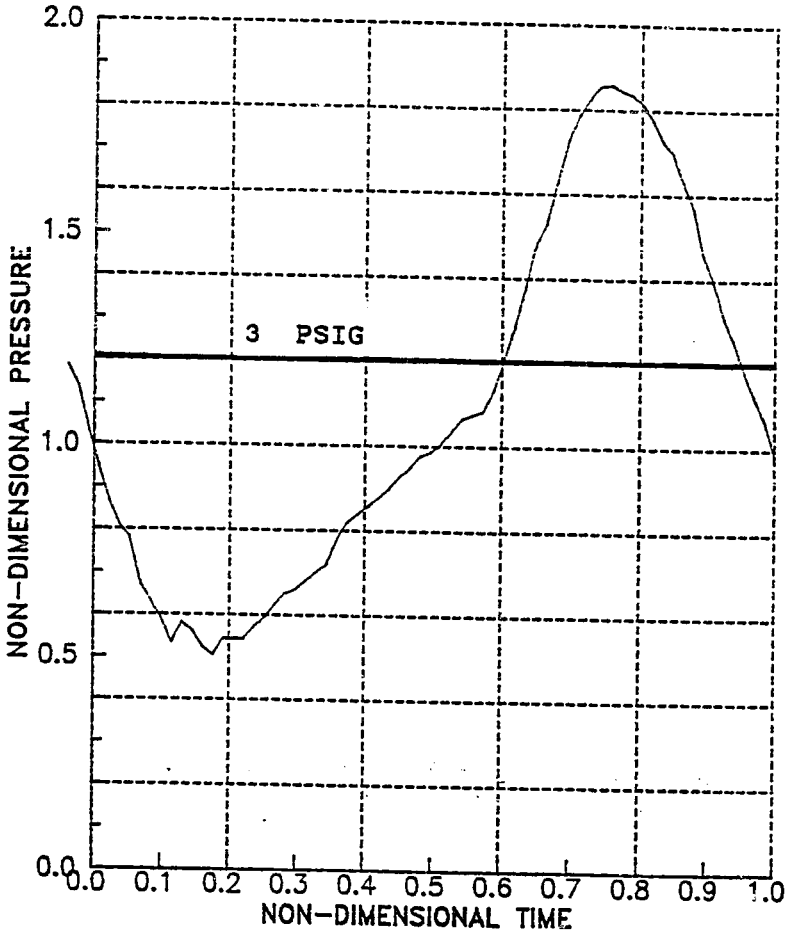

Figure 6-13 Pressure variation with time at injection location for 5.5 inch valveless pulsejet

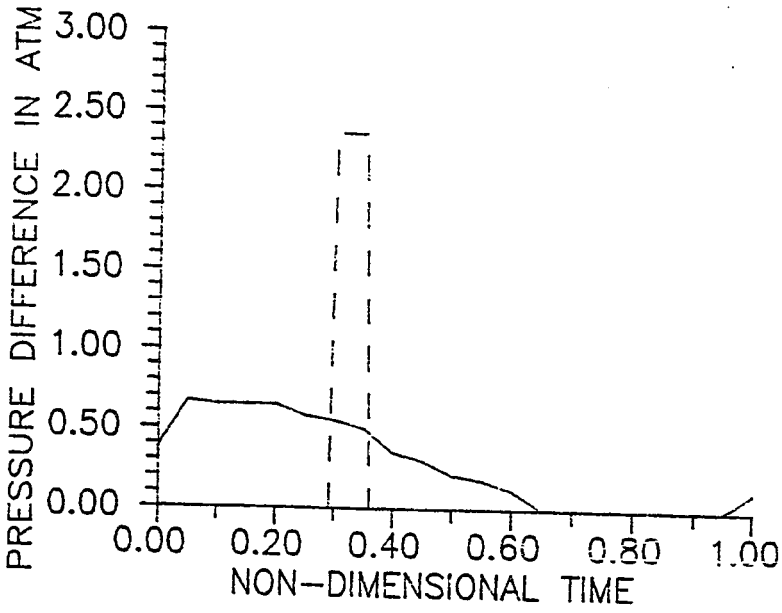

Figure 6-14 Variation of feed pressure difference for low pressure, intermittent injection and synchronous injection for one cycle

through the inlet is minimum and the diffuser mixing is minimum therefore the statistical mixture ratio is very poor.

In the Synchronous Injection Ignition injection scheme the high pressure injection insures mean fuel spray droplet size below 50 microns and provides superior penetration. In addition, injection is not begun until positive inflow has begun (a relative time of 0.3) thus providing the maximum utilization of the diffuser mixing capabilities. Thus the relative difference in the performance can be directly

attributed to the more refined fuel injection and mixing qualities of the Synchronous Injection Ignition concept.

CHAPTER 7

SUMMARY

7.1 Summary of Present Research

A numerical simulation of the unsteady gasdynamics of a standard valveless pulsejet has been developed. The model employed a quasi-one dimensional, real gas, method-of-characteristics channel flow code in conjunction with a hybrid, quasi-one dimensional mixing, constant volume combustion model. This combination produces the ability to evaluate the performance of standard valveless pulsejets and various fuel injection schemes.

The model was calibrated with existing experimental data. The results of the calibrated simulation are in good agreement with the results of other researchers. A comparison of the standard, low pressure, intermittent injection with the Synchronous Injection Ignition concept was performed to evaluate the feasibility and performance of the concept. The results indicated a significant reduction in the specific fuel consumption of the Synchronous Injection Ignition concept over the standard low pressure injection schemes.

7.2 Recommendations

The inability to define precise combustion performance in an unsteady combustion process has led to the inclusion of empirical relationships and limitations being incorporated within the present combustion model. Contributions in the analytical evaluation of this process are needed to eliminate these restrictions. The model was also limited to a one-dimensional gasdynamic model for the sake of computational time. Removal of this restriction would allow for the development of optimum combustor geometries and multiple injection schemes for increased performance. Numerical procedures need to be developed for increased speed of the simulation. Last, but certainly the most important, experimental verification of the results should be performed.

REFERENCES

1. Lorin,R., "Le propulser a echappement et l'aeroplane a grande vitesse," AEROPHILE, Vol.16, pp.332-336, 1 Sept. 1908.

2. Stodola,A., Steam and Gas Turbines, Vol.II, Peter Smith, Gloucester, Mass., pp. 1173-1270, 1945.

3. Suplee,H.H., The Gas Turbine, J.B. Lippencott Company, Philadelphia, Pa., pp. 246-250, 1910.

4. Marconnet,G., French Patent No. 412,478 (1910).

5. Schmidt,P., German Patent No. 523,655 (1930).

6. Benecke,T.H., and Quick,A.W.(editors), History of German Guided Missile Development, AGARDograph No.20, pp. 400-418, 1957.

7. Schultz-Grunow,F., Gas-Dynamic Investigation of the Pulse Jet Tube - Parts I & II, NACA TM No. 1131, February, 1947.

8. Project Squid, Princton Univ., 1943-1952.

9. Schubert,W., "Design, construction, and testing of a 6-inch valveless resojet," Naval Eng. Expt. Sta., Rept. ESS-B-5350As(b), 1944.

10. Rudinger,G., Wave Diagrams for NonSteady Flow in Ducts, VanNostrand Company,Inc., New York, 1954.

11. Bretin,J.P., "Quelques proprites de la combustion pulsatorie," in Selected Combustion Problems, Butterworths, 1954.

12. Foa,J.V., Elements of Flight Propulsion, John Wiley & Sons, New York, pp. 378-381, 1960.

13. Barrere,M. et al, "Utilisation D'un Pulsoreacteur Pour Un Classement Rapide Des Combustibles," La Recherche Aeronautique No. 37, pp. 21-28, Janvier-Fevrier 1954.

14. Lockwood,R.M., "Low Cost Pulse-Reactor VTOL Engines For Unlimited Terrain Freedom," Hiller Aircraft Co. Rept. 64-ENV-4, 1964.

15. Lockwood,R.M., "Pulse-Reactor Lift-Propulsion Engine Permits Unlimited Terrain Freedom," AIAA Paper, 1st Annual Meeting and Technical Display, 29 June- 2 July, 1964, Washington, D.C.

16. Tharratt,C.N., "The Propulsive Duct", Aircraft Engineering, pp. 332-337, 359-371, Nov.-Dec., 1965.

17. Kentfield,J.A.C., "Valveless Pulsejets and Allied Devices for Low Thrust, Subsonic, Propulsion Applications", AGARD CP-307, pp. 10-1 to 10-11.

18. Cornje,J.S., "An Experimental and Theoretical Study, Including Frictional and Heat Transfer Effects, of Pulsed Pressure-Gain Combustors", Ph.D. Dissertation, University of Calgary, Calgary, Alberta, Canada, 1979.

19. Kinsler,L.E. and Frey,A.R., Fundamentals of Acoustics, 2nd Edition, John Wiley & Sons, Inc.,New York, 1962.

20. Binder,R.C., Advanced Fluid Dynamics and Fluid Machinery, Prentice Hall, Inc.,New York, 1951.

21. Lancaster,O.E.(editor), Jet Propulsion Engines, Princton University Press, 1959.

22. Tsien,H.S.(editor), Jet Propulsion, California Institute of Technology, 1946.

23. Wilson,D.R. and Stewart,C.S., "Analysis of Transient MHD Channel Flows by a Hybrid Lax-Wendroff Method-of-Characteristics Computer Code," 20th Symposium of Engineering Aspects of Magnetohydrodynamics, University of California, Irvine, California, June, 1982.

24. Shapiro,A.H., The Dynamics and Thermodynamics of Compressible Fluid Flow, Vol.II, Ronald Press Co., New York, 1954.

25. Lee.,Y.M., "Transient Analysis of Magnetohydrodynamic Generator Flow Trains", MSAE Thesis, University of Texas at Arlington, Arlington, Texas, 1982.

26. White,F.M., Viscous Fluid Flow, Kingsport Press, Inc., New York, 1974.

27. Zucrow,M.J. and Hoffman,J.D., Gas Dynamics Vol. I & II, John Wiley & Sons, New York, 1977.

28. Sanford,G. and McBride,B.J., "Computer Program for Calculation of Complex Chemical Equilibrium Compositions, Rocket Performance, Incident and Reflected Shocks, and Chapman-Jouquet Detonations", NASA SP-273,1971.

29. Wilson,D.R., Stewart,C.S., and Lee,Y.M.,"MHD Generator Off-Design Performance and NOx Chemical Kinetics Analysis", NASA/DOE Grant NSG 3255 (Supplement 2 and 3) Final Report, Aerospace Engineering Dept., The University of Texas at Arlington, Arlington, Texas, July, 1982.

30. Svehla,R.A. and McBride,B.J., "FORTRAN IV Computer Program for Calculation of Thermodynamic and Transport Properties of Complex Chemical Systems", NASA TN-D-7056, January, 1973.

31. Salas,M.D., "Shock Fitting Method for Complicated Two-Dimensional Supersonic Flow", AIAA Journal, Vol. 14, No. 5, pp. 583-588, May, 1976.

32. Chapman,D.L., "On the rate of explosions in gases", Phil. Mag., (5), Vol. 47, p.90, 1899.

33. Jouguet,E., "Sur la propagation des recations chimiques dans les gaz", J. Math Pures et Appliquees, 6th Series, 1905-06.

34. Foa,J.V. and Rudinger,G., "On the addition of heat to a gas flowing in a pipe at supersonic speeds", Cornell Aeronautical Lab., Rept. No. HF-534-A-2, Feb. 1949.

35. AGARD Conference Proceedings No. 275, Combustion Modeling, 1979.

36. Longwell,J.P. and Weiss,M.A., "High Temperature Reaction Rates in Hydrocarbon Combustion", I.& E.C. 47, No. 8, p. 1634.

37. Spalding,D.B., Pratt,D.T., Elgobashi,S. and Srivatsa, S.K., "Unsteady Combustion of Fuel Spray in Jet Engine Afterburners", ISABE, Munich, March 1976, p. 447.

38. Schetz,J.A., Injection and Mixing in Turbulent Flows, AIAA, 1980.

39. Smith,D.E., "FORTRAN Program for the Analysis of Valveless Pulsejets", Aero.Eng.Res. Rept. No. 87-1, 1987.

40. Lockwood,R.M., "Summary Report on Investigation of Miniature Valveless Pulsejets", TRECOM Tech.Rept. 64-20, U. S. Army, February, 1964.